The Journal of Toxicological Sciences (J. Toxicol. Sci.)
Vol.41, No.2, 207-215, 2016

Original Article

Tributyltin induces G2/M cell cycle arrest via NAD$^+$-dependent isocitrate dehydrogenase in human embryonic carcinoma cells

Miki Asanagi[1,2,*], Shigeru Yamada[1,*], Naoya Hirata[1], Hiroshi Itagaki[2], Yaichiro Kotake[3], Yuko Sekino[1] and Yasunari Kanda[1]

[1]*Division of Pharmacology, National Institute of Health Sciences, 1-18-1 Kamiyoga, Setagaya-ku, Tokyo 158-8501, Japan*
[2]*Faculty of Engineering, Department of Materials Science and Engineering, Yokohama National University, 79-5 Tokiwadai, Hodogaya-ku, Yokohama, Kanagawa 240-8501, Japan*
[3]*Department of Xenobiotic Metabolism and Molecular Toxicology, Graduate School of Biomedical and Health Sciences, Hiroshima University, 1-2-3 Kasumi, Minami-ku, Hiroshima 734-8553, Japan*

(Received November 16, 2015; Accepted December 28, 2015)

ABSTRACT — Organotin compounds, such as tributyltin (TBT), are well-known endocrine-disrupting chemicals (EDCs). We have recently reported that TBT induces growth arrest in the human embryonic carcinoma cell line NT2/D1 at nanomolar levels by inhibiting NAD$^+$-dependent isocitrate dehydrogenase (NAD-IDH), which catalyzes the irreversible conversion of isocitrate to α-ketoglutarate. However, the molecular mechanisms by which NAD-IDH mediates TBT toxicity remain unclear. In the present study, we examined whether TBT at nanomolar levels affects cell cycle progression in NT2/D1 cells. Propidium iodide staining revealed that TBT reduced the ratio of cells in the G1 phase and increased the ratio of cells in the G2/M phase. TBT also reduced cell division cycle 25C (cdc25C) and cyclin B1, which are key regulators of G2/M progression. Furthermore, apigenin, an inhibitor of NAD-IDH, mimicked the effects of TBT. The G2/M arrest induced by TBT was abolished by NAD-IDHα knockdown. Treatment with a cell-permeable α-ketoglutarate analogue recovered the effect of TBT, suggesting the involvement of NAD-IDH. Taken together, our data suggest that TBT at nanomolar levels induced G2/M cell cycle arrest via NAD-IDH in NT2/D1 cells. Thus, cell cycle analysis in embryonic cells could be used to assess cytotoxicity associated with nanomolar level exposure of EDCs.

Key words: Embryonic carcinoma cells, Tributyltin, Cell cycle, Isocitrate dehydrogenase

INTRODUCTION

Organotin compounds, such as tributyltin (TBT) are typical environmental contaminants and are categorized as endocrine-disrupting chemicals (EDCs), which cause neurodevelopmental defects including behavioral abnormality and teratogenicity (Dopp *et al.*, 2004; Gårdlund *et al.*, 1991). Although the use of TBT has already been restricted, butyltin compounds, including TBT, can still be found in human blood at concentrations between 50 and 400 nM. There is still concern about TBT toxicity for human health (Whalen *et al.*, 1999).

Several studies have revealed that TBT activates retinoid X receptor (RXR) and/or peroxisome proliferator-activated receptor γ (PPARγ) (Kanayama *et al.*, 2005). TBT at nanomolar levels has the ability to bind with higher affinity than the intrinsic ligands and these genomic transcriptional activations have been reported to mediate neurodevelopmental defects in *Xenopus* (Yu *et al.*, 2011). In contrast, TBT elicits non-genomic pathway in mature rat neurons and brain tissues at nearly micromolar levels. For instance, TBT induces neuronal death by inhibiting mammalian target of rapamycin (mTOR) in rat cortical neurons (Nakatsu *et al.*, 2010). TBT also induces neuronal degeneration via the generation of reactive oxygen species along with marked reduction of GSH/GSSG levels in the rat brain (Mitra *et al.*, 2013).

Cell stress is known to trigger a checkpoint that arrests cells in the G1 or G2 phase (Gabrielli *et al.*, 2012). The cell cycle is tightly regulated by spatial and temporal

Correspondence: Yasunari Kanda (E-mail: kanda@nihs.go.jp)
*These authors equally contributed to this work.

expression of cell cycle proteins and divided into p53-dependent and p53-independent regulations (Shackelford *et al.*, 1999). In the p53-independent regulations, cdc25C phosphatase, a mitotic inducer, plays a central role in G2/M phase regulation. Cdc25C activates cyclin B1/cyclin-dependent kinase (Cdk) 1 complex, which triggers mitosis (Donzelli and Draetta, 2003) and cyclin B1 accumulates during the S and G2 phases, followed by nuclear translocation and association with Cdk1. Protein levels of these cell cycle regulators are strictly regulated during cell cycle progression. Ultraviolet irradiation or toxic drugs are known to cause G2 arrest by the inactivation of cyclin B1/Cdk1 via p53 induction followed by the upregulation of p21, a Cdk inhibitor and/or cdc25C downregulation by degradation (Chaudhary *et al.*, 2013; Kawabe, 2004; Nam *et al.*, 2010; Ouyang *et al.*, 2009).

We have previously reported that nanomolar levels of TBT induce growth arrest of neuronal precursor NT2/D1 cells as a model of neurodevelopmental stage (Yamada *et al.*, 2013). We found that TBT causes growth arrest via mitochondrial NAD^+-dependent isocitrate dehydrogenase (NAD-IDH), which catalyzes the irreversible conversion of isocitrate to α-ketoglutarate in the tricarboxylic acid (TCA) cycle (Yamada *et al.*, 2014). Based on these observations, we hypothesized that nanomolar levels of TBT could also affect cell cycle progression via NAD-IDH in NT2/D1 cells.

In the present study, we investigated the effect of TBT on cell cycle progression in NT2/D1 cells. We found that exposure to 100 nM TBT reduced the protein levels of cell cycle regulators and induced G2/M cell cycle arrest through an NAD-IDH-dependent mechanism. Thus, cell cycle regulation via NAD-IDH is a novel target of TBT-induced toxicity in human embryonic carcinoma cells.

MATERIALS AND METHODS

Cell culture

NT2/D1 cells were obtained from the American Type Culture Collection (Manassas, VA, USA). The cells were cultured in Dulbecco's modified Eagle's medium (DMEM; Sigma-Aldrich, St. Louis, MO, USA) supplemented with 10% fetal bovine serum (FBS; Biological Industries, Ashrat, Israel) and 0.05 mg/mL penicillin-streptomycin mixture (Life Technologies, Carlsbad, CA, USA) at 37°C in 5% CO_2.

Cell cycle analysis

The cells were trypsinized and harvested in phosphate buffered saline. Then the cells were resuspended in 70% ethanol for 30 min at -20°C. The fixed cells were collected by centrifugation and resuspended in propidium iodide (PI)/RNase Staining Buffer (BD Biosciences, San Jose, CA, USA) followed by incubation at room temperature for 30 min in the dark. Cell cycle distribution was determined by flow cytometric analysis of the DNA content using the BD FACS Aria II system (BD Biosciences). Data were analyzed by Modfit LT 4.0 (Verity Software House, Topsham, ME, USA).

Real-time PCR

Total RNA was extracted from NT2/D1 cells using TRIzol reagent (Life Technologies), and quantitative real-time reverse transcription (RT)-PCR was performed with QuantiTect SYBR Green RT-PCR Kit (QIAGEN, Valencia, CA, USA) using an ABI PRISM 7900HT sequence detection system (Applied Biosystems, Foster City, CA, USA) as previously reported (Hirata *et al.*, 2014). The relative change in transcript amounts was normalized to the expression levels of glyceraldehyde-3-phosphate dehydrogenase (GAPDH). The following primer sequences were used for real-time PCR analysis: human cdc25C: forward, 5′-AGGCAGCCTTGAGTTGCATAGAGA-3′, reverse, 5′-AGAGTTGGCTGGCTTGTGAGAAGA-3′;humancyclin B1:forward,5′-CGGGAAGTCACTGGAAACAT-3′,reverse, 5′-AAACATGGCAGTGACACCAA-3′; human GAPDH: forward, 5′-GTCTCCTCTGACTTCAACAGCG-3′, reverse, 5′-ACCACCCTGTTGCTGTAGCCAA-3′.

Western blot analysis

Western blot analysis was performed as previously reported (Kanda *et al.*, 2011). Briefly, cells were lysed with Cell Lysis Buffer (Cell Signaling Technology, Danvers, MA, USA). The proteins were then separated by sodium dodecyl sulfate-polyacrylamide gel electrophoresis (SDS-PAGE) and electrophoretically transferred to Immobilon-P membrane (Millipore, Billerica, MA, USA). The membranes were probed with an anti-cdc25C monoclonal antibody (1:1,000; Cell Signaling Technology), an anti-cyclin B1 monoclonal antibody (1:1,000; Cell Signaling Technology), and an anti-GAPDH polyclonal antibody (1:2,500; Abcam, Cambridge, UK) followed by incubation with horseradish peroxidase-conjugated secondary antibodies against rabbit or mouse IgG (Cel Signaling Technology). The bands were visualized using the ECL Western Blotting Analysis System (GE Healthcare, Buckinghamshire, UK), and images were acquired using a LAS-3000 Imager (FUJIFILM UK Ltd., Systems, Bedford, UK).

NAD-IDH activity assay

NAD-IDH activity was determined using the

Isocitrate Dehydrogenase Activity Colorimetric Assay Kit (Biovision, Mountain View, CA, USA), according to the manufacturer's instructions. Briefly, NT2/D1 cells were lysed in an assay buffer provided in the kit. The lysate was centrifuged at 14,000 *g* for 15 min, and the cleared supernatant was used for the assay.

NAD-IDHα knockdown

Knockdown studies were performed using NAD-IDHα shRNA lentiviruses from Sigma-Aldrich (MISSION shRNA) according to the manufacturer's protocol. A scrambled hairpin sequence was used as a negative control. Briefly, the cells were infected with the viruses at a multiplicity of infection of 10 in presence of 8 μg/mL hexadimethrine bromide (Sigma-Aldrich) for 24 hr, and were then subjected to selection with 0.5 μg/mL puromycin for 72 hr for further functional analyses.

Chemicals and reagents

Tributyltin Chloride was obtained from Tokyo Chemical Industry (Tokyo, Japan). Tin acetate (TA), apigenin, and dimethyl α-ketoglutarate (DMKG) were obtained from Sigma-Aldrich.

Statistical analysis

All data were presented as mean ± S.D. Analysis of variance (ANOVA) followed by post hoc Tukey's test was used to analyze the data in Figs. 1C, 1D, 1E, 2A, 2B, 3C, 4E, 5A, 5B, 6A and 6B. Student's t test was used to analyze the data in Figs. 3A, 3B, 4A, 4B and 4C. P-values less than 0.05 were considered to be statistically significant.

RESULTS

Effect of TBT on cell cycle progression

We have previously found that 100 nM TBT induced growth arrest in NT2/D1 cells (Yamada *et al.*, 2013). Here we investigated whether TBT affects cell cycle progression. Exposure to 100 nM TBT for 48 hr decreased the proportion of cells in the G1 phase (51.9% decrease) and increased of the proportion of cells in the G2/M phase (79.6% increase), compared with untreated control cells (Figs. 1A-E). In contrast, TBT did not affect the proportion of cells in the S phase. Moreover, exposure to tin acetate (TA), which is less toxic, did not affect cell cycle progression. These data suggest that TBT induces G2/M cell cycle arrest in the cells.

TBT exposure reduces G2/M cell cycle regulators, cdc25C and cyclin B1

To examine the molecular mechanism by which TBT induces G2/M cell cycle arrest, we assessed the protein levels of p53, a major cell cycle regulator. We found that p53 protein level was reduced after 24 hr of TBT treatment, whereas cisplatin, which is known to cause p53-dependent G2/M cell cycle arrest (Pani *et al.*, 2007), increased p53 levels (Supplementary Fig. 1). Since we could not observe p53-dependency in TBT-induced G2/M cell cycle arrest, we assessed cdc25C and its downstream factor, cyclin B1, which are also involved in G2/M progression of cell cycle. Western blot analysis revealed that cdc25C and cyclin B1 protein levels were reduced after 24 hr of TBT treatment (Fig. 2A). In contrast, exposure to TA did not affect cdc25C and cyclin B1 protein levels. Equal GAPDH protein expression levels were confirmed as a loading control. Next, we assessed the gene expression of cdc25C and cyclin B1. However, real-time PCR analysis showed that gene expression was not significantly altered by TBT exposure for both 24 and 48 hr (Fig. 2B). These data suggest that TBT-induced G2/M cell cycle arrest is caused by reduction of cdc25C and cyclin B1 proteins.

TBT induces G2/M cell cycle arrest via NAD-IDH

To investigate the molecular mechanisms by which cdc25C is degraded and G2/M cell cycle arrest is induced, we examined the effect of the PPARγ agonist rosiglitazone (RGZ), which is the genomic target of TBT. We found that RGZ did not induce G1 phase reduction and G2/M phase increase (Figs. 3A and B). RGZ at 100 nM induced PPARγ gene expression at similar level to 100 nM TBT in NT2/D1 cells (Fig. 3C), confirming the agonistic effect of RGZ on PPARγ expression described in previous report (Benkirane *et al.*, 2006). These data suggest that TBT induces G2/M cell cycle arrest in NT2/D1 cells through a non-genomic pathway. We next examined the involvement of the non-genomic target NAD-IDH. We used an NAD-IDH inhibitor apigenin (Arango *et al.*, 2013) at 10 μM, which reduced NAD-IDH activity to a level (22.4%) (Fig. 4A). As previously reported, 100 nM TBT had a similar inhibitory effect (24.4%; Yamada *et al.*, 2014). Treatment with apigenin (10 μM, 48 hr) decreased G1 phase ratio (58.6% decrease) and increased G2/M phase ratio (98.1% increase) (Figs. 4B and C). Similar to TBT, apigenin reduced protein expression of cdc25C and cyclin B1 without affecting gene expression (Figs. 4D and E). To further confirm the effect of apigenin, we performed knockdown (KD) experiments of NAD-IDHα, the catalytic subunit of NAD-IDH, using lentivirus-delivered shRNAs. Real-time PCR analysis showed that KD efficiency was approximately 40% (Yamada *et al.*, 2014). We could not obtain more highly KD cells because of cell

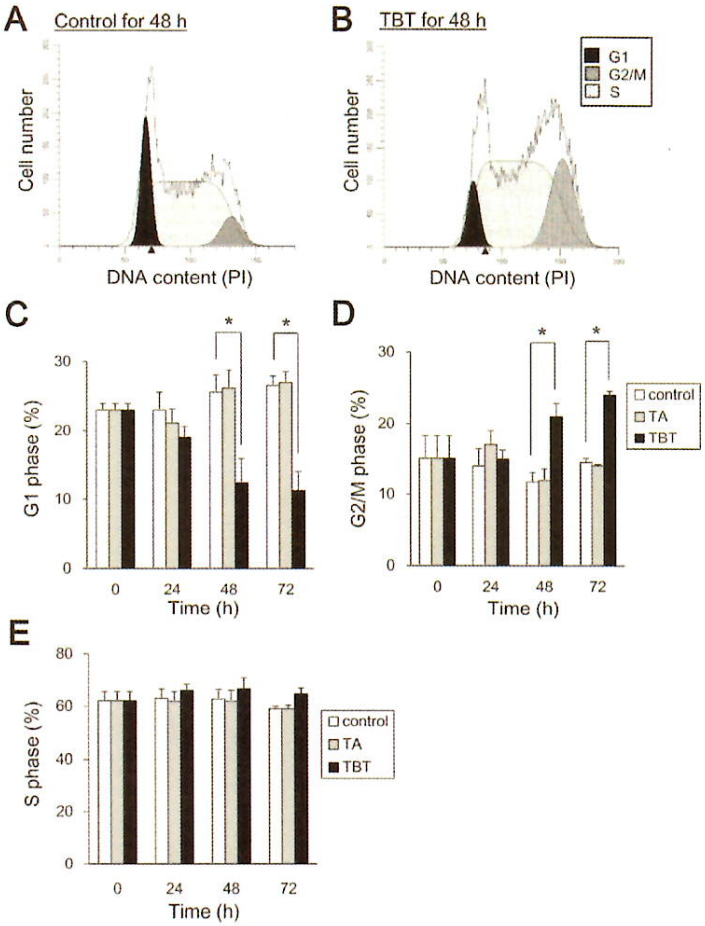

Fig. 1. Effect of TBT on cell cycle progression in NT2/D1 cells. Cells were exposed to 100 nM TA or TBT for 24, 48 or 72 hr. Cells were stained with propidium iodide (PI). Cell cycle distribution was determined by flow cytometric analysis of the DNA content on BD FACS Aria II. Representative cell cycle data in control (A) and TBT (B)-treated cells. The area ratio of G1 (C), G2/M (D) and S (E) phases was determined by Modfit LT 4.0. Data represent mean ± S.D. (n = 3). *P < 0.05.

death. Due to partial KD of the NAD-IDHα gene, NAD-IDH activity decreased by 22%, which is comparable to its decreased levels by TBT. In our previous studies, we observed that NAD-IDHα KD recovered the inhibitory effect of TBT on ATP content (Yamada *et al.*, 2014). This might be because the TBT target NAD-IDHα was already inhibited by shRNA and further inhibition by TBT was not observed in the knockdown cells. Similar to these data, NAD-IDHα KD abolished the TBT-induced G1 phase reduction and G2/M phase increase (Figs. 5A and B), suggesting the involvement of NAD-IDH on TBT effects. NAD-IDHα KD tended to decrease the proportion of cells in the G1 phase (24.1% ± 0.55 to 23.2% ± 0.34) and increase the proportion of cells in the G2/M phase (17.5% ± 1.6 to 20.3% ± 0.62), compared with control (Figs. 5A and B). Moreover, NAD-IDHα KD also abolished the TBT-induced reduction of cdc25C and cyclin B1 proteins (Fig. 5C). NAD-IDHα KD reduced the basal levels of cdc25C and cyclin B1 proteins, compared with control (Fig. 5C). These data suggest that NAD-IDH mediates TBT-induced G2/M cell cycle arrest in NT2/D1 cells. To further confirm the involvement of NAD-IDH, we treated the cells with dimethyl α-ketoglutarate (DMKG), a cell-permeable analog of α-ketoglutarate (Willenborg *et al.*, 2009). Incubation with DMKG prevented TBT-induced G2/M cell cycle arrest in NT2/D1 cells and

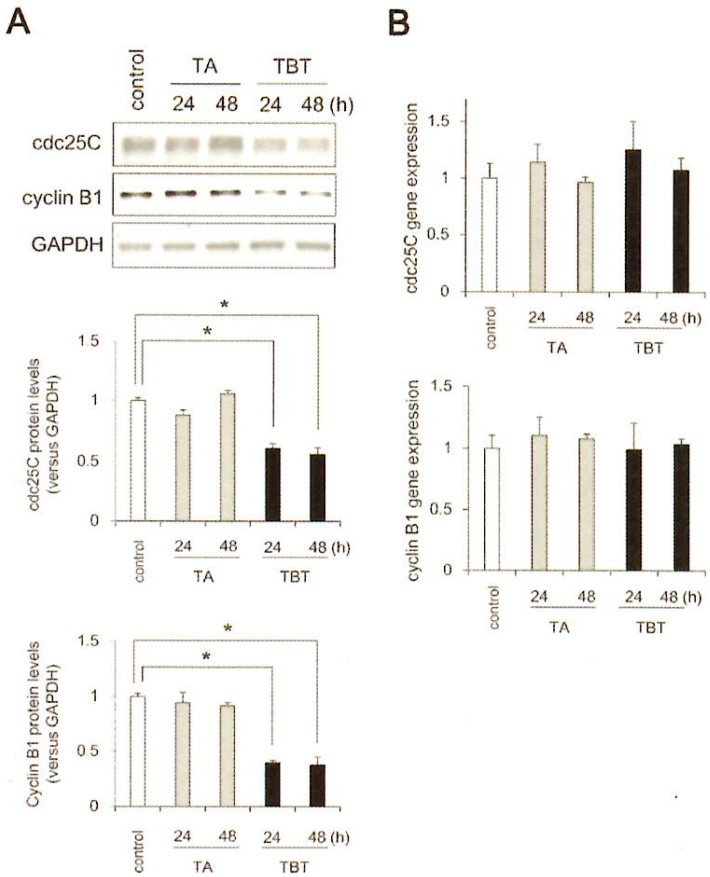

Fig. 2. Effect of TBT on expression levels of G2/M cell cycle regulators in NT2/D1 cells. After TBT exposure for 24 and 48 hr, protein expression was analyzed by western blot using anti-cdc25C, cyclin B1, or GAPDH antibodies (A). After TBT exposure for 24 or 48 hr, the expression of G2/M cell cycle regulators was analyzed by real time PCR (B). The gene expression was not significantly altered by TBT exposure. Data represent mean ± S.D. (n = 3).

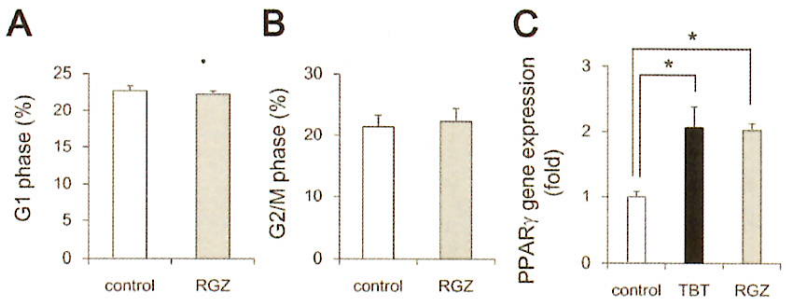

Fig. 3. Effect of RGZ on cell cycle progression in NT2/D1 cells. After RGZ exposure for 48 hr, cells were stained with propidium iodide (PI). The cell cycle distribution was determined by flow cytometric analysis of the DNA content using BD FACS Aria II. The ratio of G1 (A) and G2/M (B) phases was determined by Modfit LT 4.0. After exposure to TBT or RGZ, the expression of PPARγ was analyzed by real time PCR (C). The gene expression was comparably increased upon TBT or RGZ exposure. Data represent mean ± S.D. (n = 3). *P < 0.05.

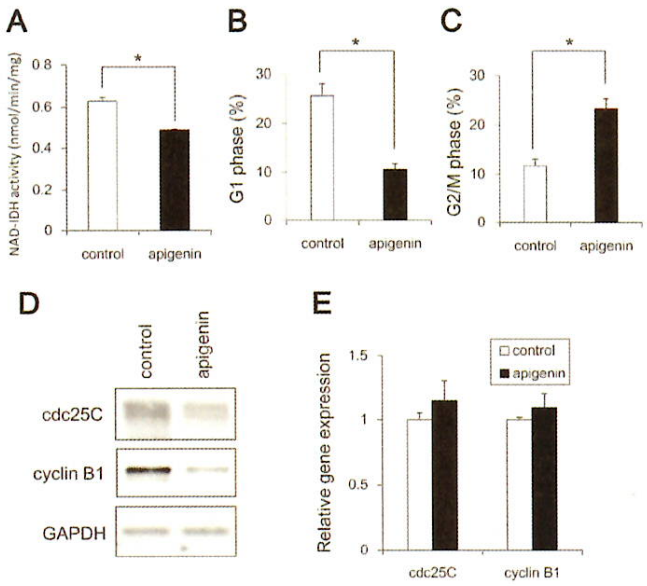

Fig. 4. Effect of apigenin on cell cycle progression in NT2/D1 cells. Cells were exposed to 10 μM apigenin for 24 hr and then determined NAD-IDH activity (A). Moreover, after exposure to apigenin for 48 hr, the cell cycle distribution was determined by flow cytometric analysis of the DNA content using BD FACS Aria II. The ratio of G1 (B) and G2/M (C) phases was determined by Modfit LT 4.0. The protein expressions in the cell lysate were analyzed by western blot using anti-cdc25C, cyclin B1, or GAPDH antibodies (D). The expression of G2/M cell cycle regulators was analyzed by real time PCR (E). The gene expression was not significantly altered upon apigenin exposure. Data represent mean ± S.D. (n = 3). *P < 0.05.

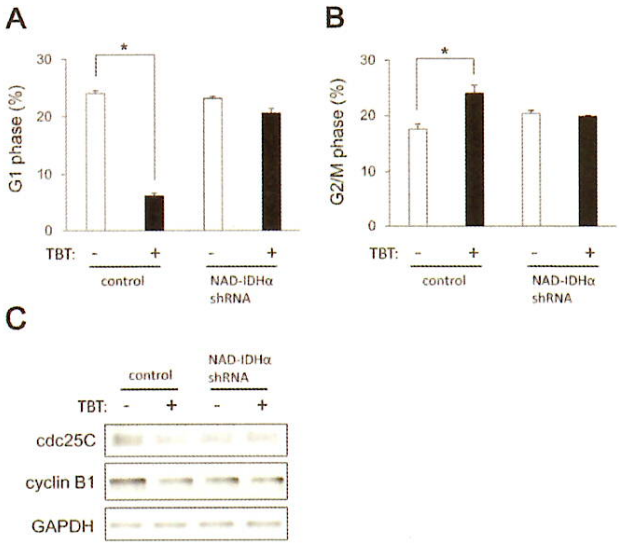

Fig. 5. Effect of NAD-IDH knockdown on cell cycle progression in NT2/D1 cells. Cells were infected with lentiviruses to express a shRNA against NAD-IDHα or a scrambled sequence shRNA (control). The infected cells were subjected to selection with 0.5 μg/mL puromycin for 72 hr and were then exposed to TBT at 100 nM for 48 hr. After staining with PI, cell cycle distribution was determined by flow cytometric analysis of the DNA content using BD FACS Aria II. The ratio of G1 (A) and G2/M (B) phases was analyzed by Modfit LT 4.0. The protein expressions in cell lysates were analyzed by western blot using anti-cdc25C, cyclin B1, or GAPDH antibodies (C). Data represent mean ± S.D. (n = 3). *P < 0.05.

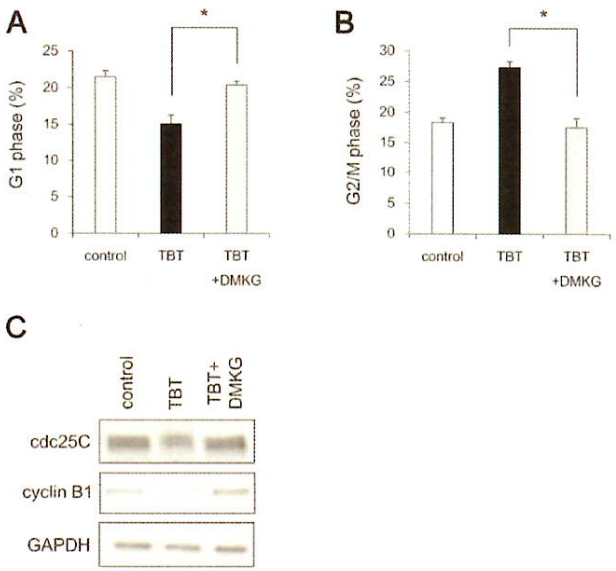

Fig. 6. Effect of dimethyl α-ketoglutarate (DMKG) on TBT-induced G2/M cell cycle arrest in NT2/D1 cells. Cells were exposed to 100 nM TBT and 7 mM DMKG for 48 hr. Cells were then stained with propidium iodide (PI) and cell cycle distribution was determined by flow cytometric analysis of the DNA content using BD FACS Aria II. The ratio of G1 (A) and G2/M (B) phases was analyzed by Modfit LT 4.0. Next, the protein expressions in cell lysates were analyzed by western blot using anti-cdc25C, cyclin B1, or GAPDH antibodies (C). Data represent mean ± S.D. (n = 3). *P < 0.05.

recovered the ratio of G1 and G2/M phases to the basal level (Figs. 6A and B). DMKG treatment also recovered TBT-induced protein reduction of cdc25C and cyclin B1 (Fig. 6C). Taken together, these data suggest that NAD-IDH mediates TBT-induced G2/M cell cycle arrest via cdc25C reduction in NT2/D1 cells.

DISCUSSION

Our data suggest that nanomolar TBT levels induce G2/M cell cycle arrest through the protein reduction of cdc25C and thereafter cyclin B1 (Figs. 1 and 2). Since the protein expression of p53 is decreased after TBT exposure, TBT-induced G2/M cell cycle arrest seems to be p53 independent. Consistent with our data, recent study has reported that nearly micromolar TBT levels induce G2/M cell cycle arrest in human amniotic cells via protein phosphatase (PP) 2A inhibition-mediated extracellular-signal-regulated kinase (ERK) inactivation (Zhang *et al.*, 2014). Since we did not observe the reduction of phospho-ERK in NT2/D1 cells after nanomolar levels of TBT exposure (data not shown), the mechanism of inducing G2 arrest may differ depending on the TBT levels and cell type. Moreover, several chemical stressors have been reported to cause G2/M cell cycle arrest through the protein reduction of cell cycle regulators (Chaudhary *et al.*, 2013; Nam *et al.*, 2010; Ouyang *et al.*, 2009). For instance, 4-Hydroxynonenal, an inducer of oxidative stress, causes DNA damage and induces G2/M cell cycle arrest in hepatocellular carcinoma HepG2 and Hep3B cells, following reduction of cdc25C and thereafter cyclin B1 proteins in a p53-independent manner (Chaudhary *et al.*, 2013). Reduction of cdc25C protein may be mediated by the ubiquitin-proteasome system in NT2/D1 cells. Cdc25C has been reported to be degraded via ubiquitination by BRCA1 during G2/M cell cycle arrest in breast cancer cell lines (Shabbeer *et al.*, 2013). During G2/M cell cycle arrest, another cell cycle regulators, such as Plk1, cdc25A and CDK1, are also known to be degraded by ubiquitin ligases, such as multi-subunit E3 ubiquitin ligases, Skp1-Cullin1-F-box Complex (SCF) or Anaphase Promoting Complex (APC) (Bassermann and Pagano, 2010). Further studies should determine whether ubiquitin ligases are involved in TBT-induced cdc25C reduction and subsequent G2/M cell cycle arrest in embryonic cells.

Our data using apigenin showed that TBT-induced G2/M cell cycle arrest is caused by NAD-IDH inhibition

(Fig. 4) and the data were verified by NAD-IDH knockdown and DMKG experiments (Figs. 5, 6). We used apigenin as a NAD-IDH inhibitor. We also confirmed the data by knockdown experiments. Since Apigenin has been reported to inhibit not only NAD-IDH but also hnRNPA2 and NF-κB (Arango *et al.*, 2013), we can not rule out the possibility that apigenin-induced G2/M cell cycle arrest was induced by other targets. Our previous report indicates that TBT induces mitochondrial dysfunction, such as impaired mitochondrial morphological dynamics and reduced ATP production via NAD-IDH in embryonic carcinoma cells (Yamada *et al.*, 2015). Considering that NAD-IDH is a mitochondrial enzyme, TBT-induced G2/M cell cycle arrest is caused by mitochondrial dysfunction through NAD-IDH inhibition. NAD-IDH catalyzes the reduction of NAD to NADH, which is oxidized by the electron transport chain and is required to generate proton electrochemical gradients across the inner mitochondrial membrane (Saraste, 1999). Thus, inhibition of NAD-IDH by TBT may reduce the NADH supply, thereby dissipating the proton electrochemical gradient. Intracellular Ca^{2+} may be also involved in mitochondrial dysfunction. Previous reports have shown that several anticancer drugs induce G2/M cell cycle arrest and apoptosis by depolarizing mitochondrial membrane potential and increasing intracellular Ca^{2+} (Fang *et al.*, 2014; Guo *et al.*, 2014). With respect to intracellular Ca^{2+}, there has been also reported that TBT induces mobilization of Ca^{2+} from intracellular stores and results in phosphorylation of MAPKs because its suppression by chelation of intracellular Ca^{2+} in human T lymphoblastoid cells (Yu *et al.*, 2000). Thus, Ca^{2+} release from depolarized mitochondria may induce G2/M cell cycle arrest after TBT exposure. Further studies should determine how the downstream signaling of NAD-IDH induces reduction of the cdc25C protein and subsequent G2/M cell cycle arrest after TBT exposure in embryonic cells.

In our previous studies, we have observed that TBT degrades mitofusin proteins and induces mitochondrial fission via the NAD-IDH inhibition. Moreover, we have also shown that TBT results in growth arrest by targeting the glycolytic systems (Yamada *et al.*, 2014). Both mitochondrial fission and glycolysis have been reported to be linked to cell cycle alterations (Yamamori *et al.*, 2015; Zhai *et al.*, 2013). Thus, we are currently investigating whether TBT-induced mitochondrial fission or glycolytic inhibition are linked to G2/M cell cycle arrest or not.

In summary, we demonstrate that TBT mediates G2/M cell cycle arrest through inhibition of NAD-IDH, representing a novel non-genomic pathway of TBT-induced toxicity (Fig. 7). These negative effects of TBT on the cell cycle could result in direct inhibition of cell growth. Thus, TBT-induced G2/M cell cycle arrest via NAD-IDH in embryonic cells may represent a novel mechanism of cytotoxicity associated with nanomolar level exposure of EDCs.

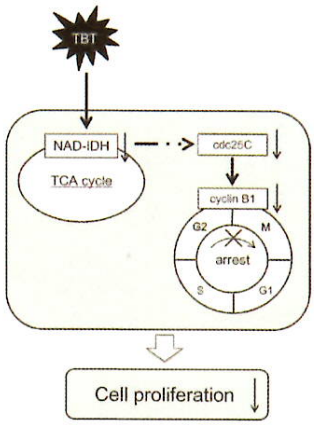

Fig. 7. Proposed model of TBT toxicity through non-genomic pathways in human embryonic carcinoma cells. Nanomolar TBT levels inhibit NAD-IDH activity. TBT induces G2/M cell cycle arrest via the protein reduction of cdc25C and its downstream target, cyclin B1. This TBT-induced G2/M cell cycle arrest may mediate cell growth inhibition.

ACKNOWLEDGMENTS

This work was supported by a Health and Labour Sciences Research Grant from the Ministry of Health, Labour and Welfare, Japan (#H25-Kagaku-Ippan-002 to Y. Kanda), a Grant-in-Aid for Scientific Research from the Ministry of Education, Culture, Sports, Science, and Technology, Japan (#26293056, #26670041 to Y. Kanda), the Research on Regulatory Harmonization and Evaluation of Pharmaceuticals, Medical Devices, Regenerative and Cellular Therapy Products, Gene Therapy Products, and Cosmetics from Japan Agency for Medical Research and development, AMED (To Y. Sekino), and a grant from the Smoking Research Foundation (Y. Kanda).

Conflict of interest---- The authors declare that there is no conflict of interest.

REFERENCES

Arango, D., Morohashi, K., Yilmaz, A., Kuramochi, K., Parihar, A., Brahimaj, B., Grotewold, E. and Doseff, A.I. (2013): Molecular basis for the action of a dietary flavonoid revealed by the com-

prehensive identification of apigenin human targets. Proc. Natl. Acad. Sci. USA, **110**, E2153-E2162.

Bassermann, F. and Pagano, M. (2010): Dissecting the role of ubiquitylation in the DNA damage response checkpoint in G2. Cell Death Differ., **17**, 78-85.

Benkirane, K., Amiri, F., Diep, Q.N., El Mabrouk, M. and Schiffrin, E.L. (2006): PPAR-gamma inhibits ANG II-induced cell growth via SHIP2 and 4E-BP1. Am. J. Physiol. Heart Circ. Physiol., **290**, H390-H397.

Chaudhary, P., Sharma, R., Sahu, M., Vishwanatha, J.K., Awasthi, S. and Awasthi, Y.C. (2013): 4-Hydroxynonenal induces G2/M phase cell cycle arrest by activation of the ataxia telangiectasia mutated and Rad3-related protein (ATR)/checkpoint kinase 1 (Chk1) signaling pathway. J. Biol. Chem., **288**, 20532-20546.

Donzelli, M. and Draetta, G.F. (2003): Regulating mammalian checkpoints through Cdc25 inactivation. EMBO Rep., **4**, 671-677.

Dopp, E., Hartmann, L.M., Florea, A.M., Rettenmeier, A.W. and Hirner, A.V. (2004): Environmental distribution, analysis, and toxicity of organometal(loid) compounds. Crit. Rev. Toxicol., **34**, 301-333.

Fang, C., Zhang, J., Qi, D., Fan, X., Luo, J., Liu, L. and Tan, Q. (2014): Evodiamine induces G2/M arrest and apoptosis via mitochondrial and endoplasmic reticulum pathways in H446 and H1688 human small-cell lung cancer cells. PLoS One, **9**, e115204.

Gabrielli, B., Brooks, K. and Pavey, S. (2012): Defective cell cycle checkpoints as targets for anti-cancer therapies. Front. Pharmacol., **3**, 9.

Gårdlund, A.T., Archer, T., Danielsen, K., Danielsson, B., Frederiksson, A., Lindquist, N.G., Lindström, H. and Luthman, J. (1991): Effects of prenatal exposure to tributyltin and trihexyltin on behaviour in rats. Neurotoxicol. Teratol., **13**, 99-105.

Guo, J., Zhao, W., Hao, W., Ren, G., Lu, J. and Chen, X. (2014): Cucurbitacin B induces DNA damage, G2/M phase arrest, and apoptosis mediated by reactive oxygen species (ROS) in leukemia K562 cells. Anticancer Agents Med. Chem., **14**, 1146-1153.

Hirata, N., Yamada, S., Shoda, T., Kurihara, M., Sekino, Y. and Kanda, Y. (2014): Sphingosine-1-phosphate promotes expansion of cancer stem cells via S1PR3 by a ligand-independent Notch activation. Nat. Commun., **5**, 4806.

Kanayama, T., Kobayashi, N., Mamiya, S., Nakanishi, T. and Nishikawa, J. (2005): Organotin compounds promote adipocyte differentiation as agonists of the peroxisome proliferator-activated receptor gamma/retinoid X receptor pathway. Mol. Pharmacol., **67**, 766-774.

Kanda, Y., Hinata, T., Kang, S.W. and Watanabe, Y. (2011): Reactive oxygen species mediate adipocyte differentiation in mesenchymal stem cells. Life Sci., **89**, 250-258.

Kawabe, T. (2004): G2 checkpoint abrogators as anticancer drugs. Mol. Cancer Ther., **3**, 513-519.

Mitra, S., Gera, R., Siddiqui, W.A. and Khandelwal, S. (2013): Tributyltin induces oxidative damage, inflammation and apoptosis via disturbance in blood–brain barrier and metal homeostasis in cerebral cortex of rat brain: an *in vivo* and *in vitro* study. Toxicology, **310**, 39-52.

Nakatsu, Y., Kotake, Y., Takai, N. and Ohta, S. (2010): Involvement of autophagy via mammalian target of rapamycin (mTOR) inhibition in tributyltin-induced neuronal cell death. J. Toxicol. Sci., **35**, 245-251.

Nam, C., Doi, K. and Nakayama, H. (2010): Etoposide induces G2/M arrest and apoptosis in neural progenitor cells via DNA damage and an ATM/p53-related pathway. Histol. Histopathol., **25**, 485-493.

Ouyang, G., Yao, L., Ruan, K., Song, G., Mao, Y. and Bao, S. (2009): Genistein induces G2/M cell cycle arrest and apoptosis of human ovarian cancer cells via activation of DNA damage checkpoint pathways. Cell Biol. Int., **33**, 1237-1244.

Pani, E., Stojic, L., El-Shemerly, M., Jiricny, J. and Ferrari, S. (2007): Mismatch repair status and the response of human cells to cisplatin. Cell Cycle, **6**, 1796-1802.

Saraste, M. (1999): Oxidative phosphorylation at the fin de siècle. Science, **283**, 1488-1493.

Shabbeer, S., Omer, D., Berneman, D., Weitzman, O., Alpaugh, A., Pietraszkiewicz, A., Metsuyanim, S., Shainskaya, A., Papa, M.Z. and Yarden, R.I. (2013): BRCA1 targets G2/M cell cycle proteins for ubiquitination and proteasomal degradation. Oncogene, **32**, 5005-5016.

Shackelford, R.E., Kaufmann, W.K. and Paules, R.S. (1999): Cell cycle control, checkpoint mechanisms, and genotoxic stress. Environ. Health Perspect., **107**, 5-24.

Whalen, M.M., Loganathan, B.G. and Kannan, K. (1999): Immunotoxicity of environmentally relevant concentrations of butyltins on human natural killer cells *in vitro*. Environ. Res., **81**, 108-116.

Willenborg, M., Panten, U. and Rustenbeck, I. (2009): Triggering and amplification of insulin secretion by dimethyl alpha-ketoglutarate, a membrane permeable alpha-ketoglutarate analogue. Eur. J. Pharmacol., **607**, 41-46.

Yamada, S., Kotake, Y., Sekino, Y. and Kanda, Y. (2013): AMP-activated protein kinase-mediated glucose transport as a novel target of tributyltin in human embryonic carcinoma cells. Metallomics, **5**, 484-491.

Yamada, S., Kotake, Y., Demizu, Y., Kurihara, M., Sekino, Y. and Kanda, Y. (2014): NAD-dependent isocitrate dehydrogenase as a novel target of tributyltin in human embryonic carcinoma cells. Sci. Rep., **4**, 5952.

Yamada, S., Kotake, Y., Nakano, M., Sekino, Y. and Kanda, Y. (2015): Tributyltin induces mitochondrial fission through NAD-IDH dependent mitofusin degradation in human embryonic carcinoma cells. Metallomics, **7**, 1240-1246.

Yamamori, T., Ike, S., Bo, T., Sasagawa, T., Sakai, Y., Suzuki, M., Yamamoto, K., Nagane, M., Yasui, H. and Inanami, O. (2015): Inhibition of the mitochondrial fission protein dynamin-related protein 1 (Drp1) impairs mitochondrial fission and mitotic catastrophe after X-irradiation. Mol. Biol. Cell, **26**, 4607-4617.

Yu, L., Zhang, X., Yuan, J., Cao, Q., Liu, J., Zhu, P. and Shi, H. (2011): Teratogenic effects of triphenyltin on embryos of amphibian (*Xenopus tropicalis*): a phenotypic comparison with the retinoid X and retinoic acid receptor ligands. J. Hazard Mater., **192**, 1860-1868.

Yu, Z.P., Matsuoka, M., Wispriyono, B., Iryo, Y. and Igisu, H. (2000): Activation of mitogen-activated protein kinases by tributyltin in CCRF-CEM cells: role of intracellular Ca(2+). Toxicol. Appl. Pharmacol., **168**, 200-207.

Zhai, X., Yang, Y., Wan, J., Zhu, R. and Wu, Y. (2013): Inhibition of LDH-A by oxamate induces G2/M arrest, apoptosis and increases radiosensitivity in nasopharyngeal carcinoma cells. Oncol. Rep., **30**, 2983-2991.

Zhang, Y., Go, Z. and Xu, L. (2014): Tributyltin induces a G2/M cell cycle arrest in human amniotic cells via PP2A inhibition-mediated inactivation of the ERK1/2 cascades. Environ. Toxicol. Pharmacol., **37**, 812-818.

Biochemical and Biophysical Research Communications 470 (2016) 300–305

Contents lists available at ScienceDirect

Biochemical and Biophysical Research Communications

journal homepage: www.elsevier.com/locate/ybbrc

Nicotine induces mitochondrial fission through mitofusin degradation in human multipotent embryonic carcinoma cells

Naoya Hirata [a, 1], Shigeru Yamada [a, 1], Miki Asanagi [a, b], Yuko Sekino [a], Yasunari Kanda [a, *]

[a] Division of Pharmacology, National Institute of Health Sciences, Japan
[b] Faculty of Engineering, Department of Materials Science and Engineering, Yokohama National University, Japan

ARTICLE INFO

Article history:
Received 5 January 2016
Accepted 10 January 2016
Available online 13 January 2016

Keywords:
Embryonic cells
Cigarette smoking
Nicotine
Mitochondrial fission
Mitofusin

ABSTRACT

Nicotine is considered to contribute to the health risks associated with cigarette smoking. Nicotine exerts its cellular functions by acting on nicotinic acetylcholine receptors (nAChRs), and adversely affects normal embryonic development. However, nicotine toxicity has not been elucidated in human embryonic stage. In the present study, we examined the cytotoxic effects of nicotine in human multipotent embryonal carcinoma cell line NT2/D1. We found that exposure to 10 μM nicotine decreased intracellular ATP levels and inhibited proliferation of NT2/D1 cells. Because nicotine suppressed energy production, which is a critical mitochondrial function, we further assessed the effects of nicotine on mitochondrial dynamics. Staining with MitoTracker revealed that 10 μM nicotine induced mitochondrial fragmentation. The levels of the mitochondrial fusion proteins, mitofusins 1 and 2, were also reduced in cells exposed to nicotine. These nicotine effects were blocked by treatment with mecamylamine, a nonselective nAChR antagonist. These data suggest that nicotine degrades mitofusin in NT2/D1 cells and thus induces mitochondrial dysfunction and cell growth inhibition in a nAChR-dependent manner. Thus, mitochondrial function in embryonic cells could be used to assess the developmental toxicity of chemicals.

1. Introduction

Growing evidence suggest that maternal smoking during pregnancy is related to adverse neurodevelopmental outcomes in the offspring, including lower intelligence quotients and deficits in learning and memory [1,2]. Nicotine is a naturally occurring alkaloid that is present in tobacco leaves and is considered to contribute to the negative effects of cigarette smoking on health [2,3]. Nicotine exerts its cellular functions by activating nicotinic acetylcholine receptors (nAChRs), which are heterodimers composed of combinations of different types of α subunit (α1–α10) and β subunit (β1–β4) [4]. α8-nAChR has not been identified in human. Recent studies have shown that nAChRs are present in a variety of cells, such as cancer cells, vascular smooth muscle, and neural cells [3–6]. Activation of nAChRs by nicotine promotes the release of various neurotransmitters (including dopamine, norepinephrine, acetylcholine, glutamate) [7]. Altered regulation of neurotransmitter levels can adversely affect key events in normal brain development, such as the formation of neural circuits and neurotransmitter systems [7,8]. Therefore, it is necessary to elucidate the cytotoxic effects of nicotine on embryonic development.

Nicotine toxicity has been reported to affect mitochondrial function both *in vitro* and *in vivo*. For example, nicotine exposure alters mitochondrial membrane potential (MMP), increases an oxidative stress, and induces apoptosis in colon adenocarcinoma HCT-116 cell [9]. Another study has shown that nicotine exposure reduced the activity of an enzyme in the pancreatic mitochondrial respiratory chain, and impaired glucose-stimulated insulin secretion in neonatal rats [10]. However, the precise mechanisms underlying the effects of nicotine on mitochondrial function remain largely unknown.

Growing evidence suggest that mitochondria undergo continuous morphological dynamics involving fusion and fission cycles. These dynamics play a key role in maintenance of normal mitochondrial functions, such as ATP production [11]. Mitochondrial fusion and fission are regulated by several GTPases. Mitofusin 1 and 2 (Mfn1, 2) and optic atrophy 1 (Opa1) induce fusion of the outer and inner mitochondrial membranes, respectively [12,13]. In contrast, dynamin-related protein 1 (Drp1) is a cytoplasmic protein that assembles into rings surrounding the outer mitochondrial

* Corresponding author. 1-18-1, Kamiyoga, Setagaya-ku, 158-8501, Japan.
E-mail address: kanda@nihs.go.jp (Y. Kanda).
[1] Equally contributed.

http://dx.doi.org/10.1016/j.bbrc.2016.01.063
0006-291X/

membrane, where it interacts with fission protein 1 (Fis1) to promote fission [14,15]. For example, pigment epithelium-derived factor is reported to improve mitochondrial function by stabilizing mitochondrial fusion in retinal pigment epithelial cells [16]. In contrast, the anti-tumor agent, doxorubicin, facilitates mitochondrial fragmentation and apoptosis by promoting Mfn2 degradation in sarcoma U2OS cells [17].

In the present study, we hypothesized a possible link between nicotine toxicity and mitochondrial function in human mulitpotent NT2/D1 cells, which have neural differentiation capability. Our results showed that exposure to 10 μM nicotine decreased intracellular ATP levels and inhibited cell growth. Moreover, nicotine exposure induced Mfn degradation and mitochondrial fragmentation via nicotinic acetylcholine receptors (nAChRs). Thus, nicotine induces toxicity through impairment of mitochondrial quality control in human NT2/D1 cells.

2. Materials and methods

2.1. Cell culture

The human multipotent embryonal carcinoma NT2/D1 cells were obtained from the American Type Culture Collection (Manassas, VA, USA). SH-SY5Y cells were obtained from European Collection of Animal Cell Culture (Salisbury, Wiltshire, UK). The cells were cultured in Dulbecco's modified Eagle's medium (DMEM; Sigma–Aldrich, St. Louis, MO, USA) supplemented with 10% fetal bovine serum (FBS; Biological Industries, Ashrat, Israel) and 0.05 mg/ml penicillin-streptomycin mixture (Life Technologies, Carlsbad, CA, USA) at 37 °C in the presence of 5% CO_2.

2.2. Cell proliferation assay

Cell viability was measured using the CellTiter 96 AQueous One Solution Cell Proliferation Assay (Promega, Madison, WI, USA), as previously described [18]. Briefly, NT2/D1 cells were seeded into 96-well plate and exposed to different concentrations of nicotine. After exposure to nicotine, One Solution Reagent was added to each well, and the plate was incubated at 37 °C for another 2 h. Absorbance was measured at 490 nm by iMark microplate reader (Bio-Rad, Hercules, CA, USA).

2.3. Measurement of intracellular ATP levels

The intracellular ATP content was measured using the ATP Determination Kit (Life Technologies), as previously described [19]. Briefly, the cells were washed and lysed with phosphate-buffered saline containing 0.1% Triton X-100. The resulting cell lysates were added to a reaction mixture containing 0.5 mM D-luciferin, 1 mM dithiothreitol, and 1.25 μg/ml luciferase and incubated for 30 min at room temperature. Luminescence was measured using a Wallac1420ARVO fluoroscan (Perkin–Elmer, Waltham, MA, USA). The luminescence intensities were normalized to the total protein content.

2.4. Assessment of mitochondrial fusion

After treatment with nicotine (10 μM, 24 h), cells were fixed with 4% paraformaldehyde and stained with 50 nM MitoTracker Red CMXRos (Cell Signaling Technology, Danvers, MA, USA) and 0.1 μg/ml 4′,6-diamidino-2-phenylindole (DAPI; Dojin, Kumamoto, Japan). Changes in mitochondrial morphology were observed using a confocal laser microscope (Nikon A1). Images (n = 3–7) of random fields were taken, and the number of cells displaying mitochondrial fusion (<10% punctiform) was counted in each image, as previously described [20]. The number of cells showing mitochondrial fission was calculated by subtracting the number of cells with mitochondrial fusion from the total cell number.

2.5. Real-time PCR

Total RNA was isolated from NT2/D1 cells using TRIzol reagent (Life Technologies), and quantitative real-time reverse transcription (RT)-PCR with QuantiTect SYBR Green RT-PCR Kit (QIAGEN, Valencia, CA, USA) was performed using an ABI PRISM 7900HT sequence detection system (Applied Biosystems, Foster City, CA, USA) as previously described [21]. The relative change in the amount of transcript was normalized to the mRNA levels of glyceraldehyde-3-phosphate dehydrogenase (GAPDH). The following primer sequences were used for real-time PCR analysis: *nAChRα1*, forward, 5′-CTGGACCTACGACGGCTCT-3′ and reverse, 5′-CGCTGCATGACGAAGTGGT-3′; *nAChRα2*, forward, 5′-ACACTTCAGACGTGGTGATTG-3′ and reverse, 5′-CCACTCCTGTTTTAGCCAGAC-3′; *nAChRα3*, forward, 5′-ACCTGTGGCTCAAGCAAATCT-3′ and reverse, 5′-GCAGGGACACGCATGAACT-3′; *nAChRα4*, forward, 5′-GGAGGGCGTCCAGTACATTG-3′ and reverse, 5′-GAAGATGCGGTCGATGACCA-3′; *nAChRα5*, forward, 5′-AGATGGAACCCTGATGACTATGGT-3′ and reverse, 5′-AAACGTCCATCTGCATTATCAAAC-3′; *nAChRα6*, forward, 5′-GGCAGGGATTCCTTCATGGG-3′ and reverse, 5′-GCCTCTCCTCAGTTGCACAG-3′; *nAChRα7*, forward, 5′-CATGGCCTTCTCGGTCTTCA-3′ and reverse, 5′-CACGGCCTCCACGAAGTT-3′; *nAChRα10*, forward, 5′-CAGATGCCTACCTACGATGGG-3′ and reverse, 5′-GGGAAGGCTGCTACATCCA-3′; *nAChRβ1*, forward, 5′-TGAGACCTCACTATCAGTACCCA-3′ and reverse, 5′-AGAACCACGACACTAAGGATGA-3′; *nAChRβ2*, forward, 5′-GGTGACAGTACAGCTTATGGTG-3′ and reverse, 5′-AGGCGATAATCTTCCCACTCC-3′; *nAChRβ3*, forward, 5′-TGCTGGTTCTCATCGTCCTTG-3′ and reverse, 5′-GCATCTTCATTTTCGGCGATTGA-3′; *nAChRβ4*, forward, 5′-CAGCTTATCAGCGTGAATGAGC-3′ and reverse, 5′-GTCAGGCGGTAATCAGTCCAT-3′; *Drp1*, forward, 5′-TGGGCGCCGACATCA-3′ and reverse, 5′-GCTCTGCGTTCCCACTACGA-3′; *Fis1*, forward, 5′-TACGTCCGCGGGTTGCT-3′ and reverse, 5′-CCAGTTCCTTGGCCTGGTT-3′; *Mfn1*, forward, 5′-GGCATCTGTGGCCGAGTT-3′ and reverse, 5′-ATTATGCTAAGTCTCCGCTCCAA-3′; *Mfn2*, forward, 5′-GCTCGGAGGCACATGAAAGT-3′ and reverse, 5′-ATCACGGTGCTCTTCCCATT-3′; *Opa1*, forward, 5′-GTGCTGCCCGCCTAGAAA-3′ and reverse, 5′-TGACAGGCACCCGTACTCAGT-3′; *GAPDH*, forward, 5′-GTCTCCTCTGACTTCAACAGCG-3′ and reverse, 5′-ACCACCCTGTTGCTGTAGCCAA-3′.

2.6. Western blot analysis

Western blot analysis was performed as previously reported [22]. Briefly, the cells were lysed with Cell Lysis Buffer (Cell Signaling Technology). The proteins were then separated by sodium dodecyl sulfate-polyacrylamide gel electrophoresis (SDS-PAGE) and electrophoretically transferred to Immobilon-P (Millipore, Billerica, MA, USA). The membranes were probed with anti-Drp1 monoclonal antibodies (1:1000; Cell Signaling Technology), anti-Fis1 polyclonal antibodies (1:200; Santa Cruz Biotechnology, Santa Cruz, CA, USA), anti-Mfn1 polyclonal antibodies (1:1000; Cell Signaling Technology), anti-Mfn2 monoclonal antibodies (1:1000; Cell Signaling Technology), anti-Opa1 monoclonal antibodies (1:1000; BD Biosciences), and anti-β-actin monoclonal antibodies (1:5000; Sigma–Aldrich). The membranes were then incubated with secondary antibodies against rabbit or mouse IgG conjugated to horseradish peroxidase (Cell Signaling Technology). The bands were visualized using the ECL Western Blotting Analysis System (GE

Healthcare, Buckinghamshire, UK), and images were acquired using a LAS-3000 Imager (FUJIFILM UK Ltd., Systems, Bedford, UK).

2.7. Chemicals and reagents

Nicotine was obtained from Wako Pure Chemicals (Osaka, Japan). Mecamylamine hydrochloride (MCA) and m-chlorophenylhydrazone (CCCP) were obtained from Sigma–Aldrich.

2.8. Statistical analysis

All data were presented as means ± S.D. ANOVA followed by post hoc Fisher test was used to analyze data in Fig. 1A and B and Figs. 2–4C. Student's *t*-test was used to analyze data in Fig. 4A. *P*-values less than 0.05 were considered to be statistically significant.

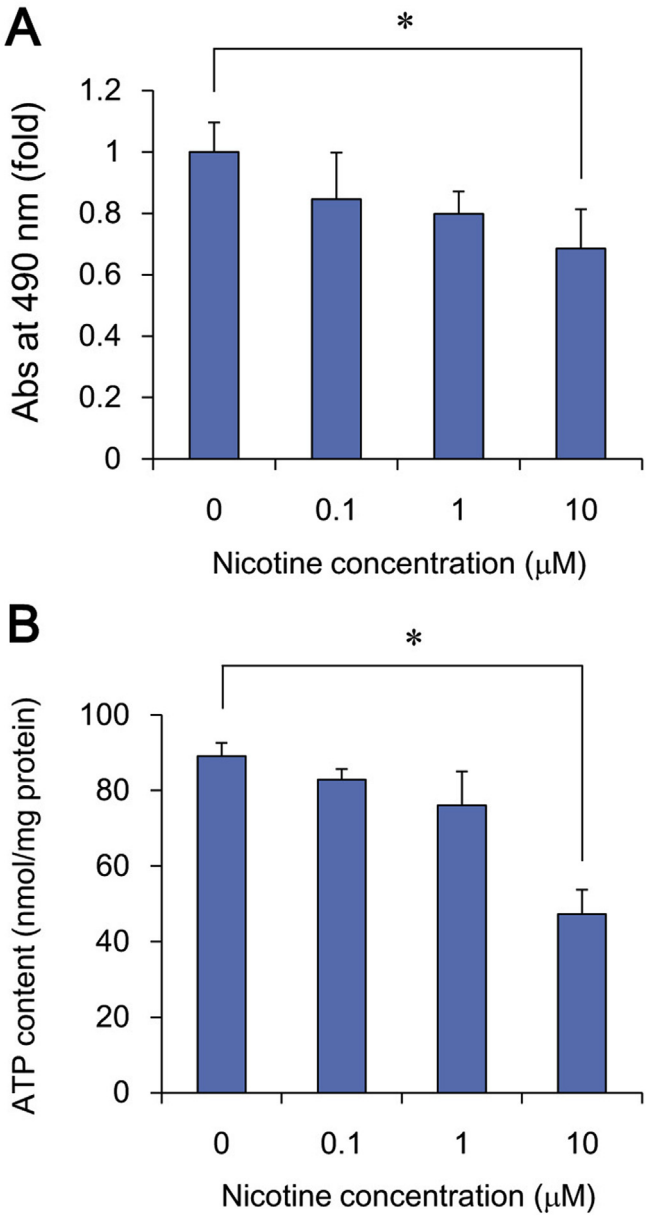

Fig. 1. Nicotine inhibits cell proliferation via intracellular ATP decrease in NT2/D1 cells. A. Cells were exposed to different concentrations of nicotine for 72 h. Cell viability was examined using the CellTiter 96 AQueous One Solution Cell Proliferation Assay. B. After treatment with different concentrations of nicotine for 24 h, intracellular ATP content was determined in cell lysates. Data represent the mean ± SD (n = 3). *P < 0.05.

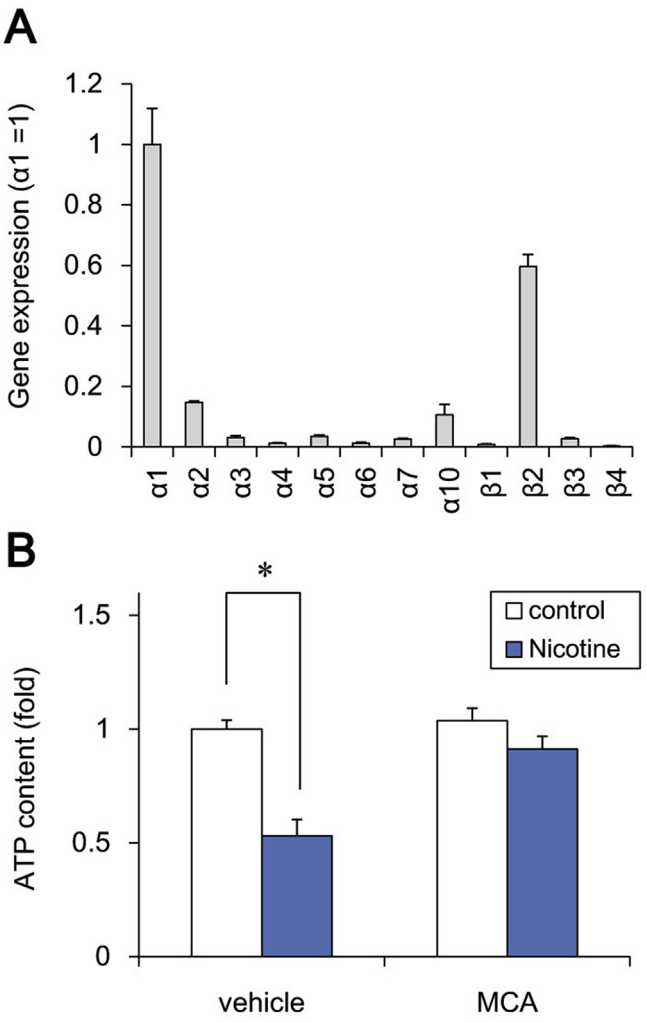

Fig. 2. Nicotine reduces intracellular ATP levels via nAChRs in NT2/D1 cells. A. Expression of AChR subtypes was analyzed by real-time PCR in NT2/D1 cells. The relative changes were determined by normalizing with GAPDH. B. After treatment with 10 μM nicotine and/or 30 μM MCA for 24 h, intracellular ATP content was determined in cell lysates. Data represent the mean ± SD (n = 3). *P < 0.05.

3. Results

3.1. Cytotoxic effects of nicotine in NT2/D1 cells

To examine the effects of nicotine on human multipotent embryonic cells, we exposed the cells to different concentrations of nicotine for 72 h and measured cell viability by MTT assay using human multipotent embryonic carcinoma NT2/D1 cells, which have an ability to differentiate into neuronal cells. We found that treatment with 10 μM nicotine significantly inhibited cell proliferation (Fig. 1A). Similarly, exposure to 10 μM nicotine significantly reduced the ATP content of the cells (Fig. 1B). To further investigate whether the nicotine effects are selective for undifferentiated cells, we used human SH-SY5Y neuroblastoma cells. We found that exposure to 10 μM nicotine had little effect on proliferation and ATP content of SH-SY5Y cells (Fig. S1).

We next examined the nAChR mRNA levels by real-time PCR and confirmed that nAChR subtypes except α9-nAChR were expressed in NT2/D1 cells (Fig. 2A). To examine whether the inhibition of ATP

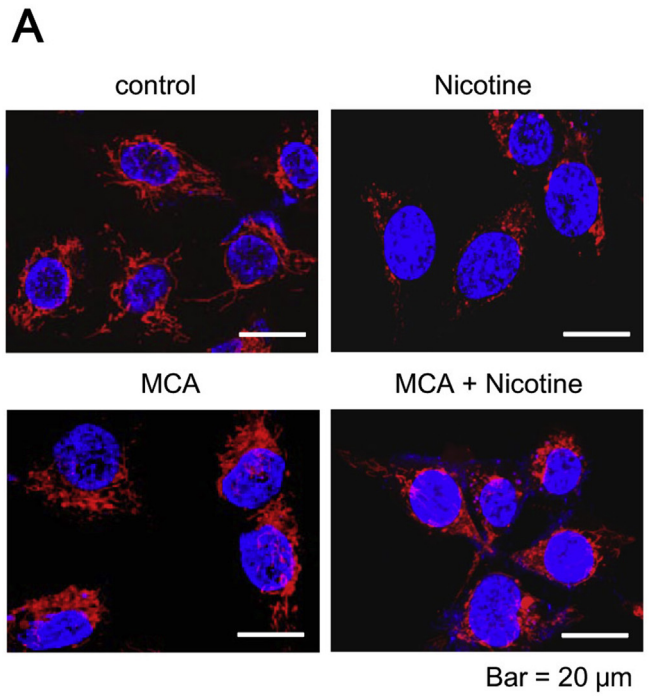

Fig. 3. Nicotine induces mitochondrial fission via nAChRs in NT2/D1 cells. A. Cells were exposed to 10 μM nicotine, in the presence or absence of 30 μM MCA, for 24 h. The cells were stained with MitoTracker Red CMXRos and DAPI and mitochondrial morphology was observed by confocal laser microscopy. Bar = 20 μm. B. The number of cells showing mitochondrial fusion (<10% punctiform) was counted in three independent captured images. The number of cells showing mitochondrial fission was calculated by subtracting the number of cells with mitochondrial fusion from the total cell number. *$P < 0.05$.

production is mediated via the nAChRs, we tested the effect of nAChR antagonist on the ATP content. As shown in Fig. 2B, a non-selective nAChR antagonist mecamylamine (MCA) abolished the nicotine-induced reduction of ATP content. MCA alone did not affect the ATP level. These data suggest that nicotine decreases the ATP content via its nAChR and inhibits cell proliferation in NT2/D1 cells.

3.2. Effects of nicotine on mitochondrial morphology in NT2/D1 cells

Mitochondrial function, including ATP production, are maintained by mitochondrial fusion and fission [11]. Since nicotine reduced intracellular ATP levels, we next focused on the mitochondrial dynamics in NT2/D1 cells. Nicotine exposure (10 μM, 24 h) significantly increased the number of fragmented mitochondria with punctate morphology, as compared to the level observed in untreated control cells (Fig. 3). Moreover, MCA abolished this nicotine-induced mitochondrial fragmentation (Fig. 3). MCA alone did not affect mitochondrial dynamics. In contrast to NT2/D1 cells, nicotine did not significantly affect the mitochondrial dynamics in SH-SY5Y neuroblastoma cells (Fig. S1). These results suggest that nicotine induces mitochondrial fission via nAChRs in NT2/D1 cells.

3.3. Nicotine reduces Mfn1 and Mfn2 protein levels in NT2/D1 cells

To examine the molecular mechanism by which nicotine induces mitochondrial fragmentation, we assessed its effects on mitochondrial fission (Fis1, Drp1) and fusion genes (Mfn1, Mfn2, Opa1). Real-time PCR analysis showed that each gene expression was not significantly altered by nicotine exposure (Fig. 4A). Interestingly, western blot analysis revealed that nicotine did significantly decrease the levels of Mfn1 and Mfn2 proteins (Fig. 4B and C). In contrast, the levels of other proteins, including Fis1, Drp1, and Opa1, were not affected by nicotine. These data suggest that nicotine-induced mitochondrial fragmentation is caused by the degradation of Mfn1 and Mfn2 proteins.

4. Discussion

In the present study, we demonstrated that exposure to micromolar levels of nicotine impairs mitochondrial quality control in human multipotent embryonic carcinoma cells. Exposure to nicotine induces nAChR-dependent degradation of Mfn1 and Mfn2, thereby promoting mitochondrial fragmentation. These negative nAChR-mediated effects of nicotine on mitochondrial quality control could inhibit ATP production and cell viability.

Undifferentiated embryonic cells may tend to be sensitive to the growth inhibitory effects of nicotine, whereas proliferative and protective effects of nicotine have been described in more developed somatic cells [23–27]. Our studies showed that treatment with 10 μM nicotine reduces cell growth in human embryonic cells (Fig. 1), whereas the growth of human neuroblastoma SH-SY5Y cells is not affected (Fig. S1). Previous study has also shown that exposure to more than 1.8 μM nicotine inhibits cell adhesion and induces apoptosis in human embryonic stem cells [28]. The concentrations of nicotine tested in our study were relevant to the circulating levels of nicotine in cigarette smokers, which have been reported to range from 10 nM to 10 μM [29]; these have the potential to inhibit the growth of embryonic cells. In contrast to these growth inhibitory effects, nicotine is known to stimulate the proliferation of hematopoietic and neuronal progenitors [23–25]. In addition, nicotine is reported to protect rat basal forebrain neurons or rat hippocampal neurons from the cytotoxicity of β-amyloid protein [26,27]. Taken together, nicotine effects in undifferentiated embryonic cells contains different mechanisms from developed somatic cells. Therefore, further studies are required to elucidate the mechanism of cell stage-specific effects using embryonic and differentiated cells.

Our data suggest that nicotine induces mitochondrial fission through the degradation of Mfn1 and Mfn2 (Figs. 3 and 4). Consistent with this finding, chemical stressors have been reported

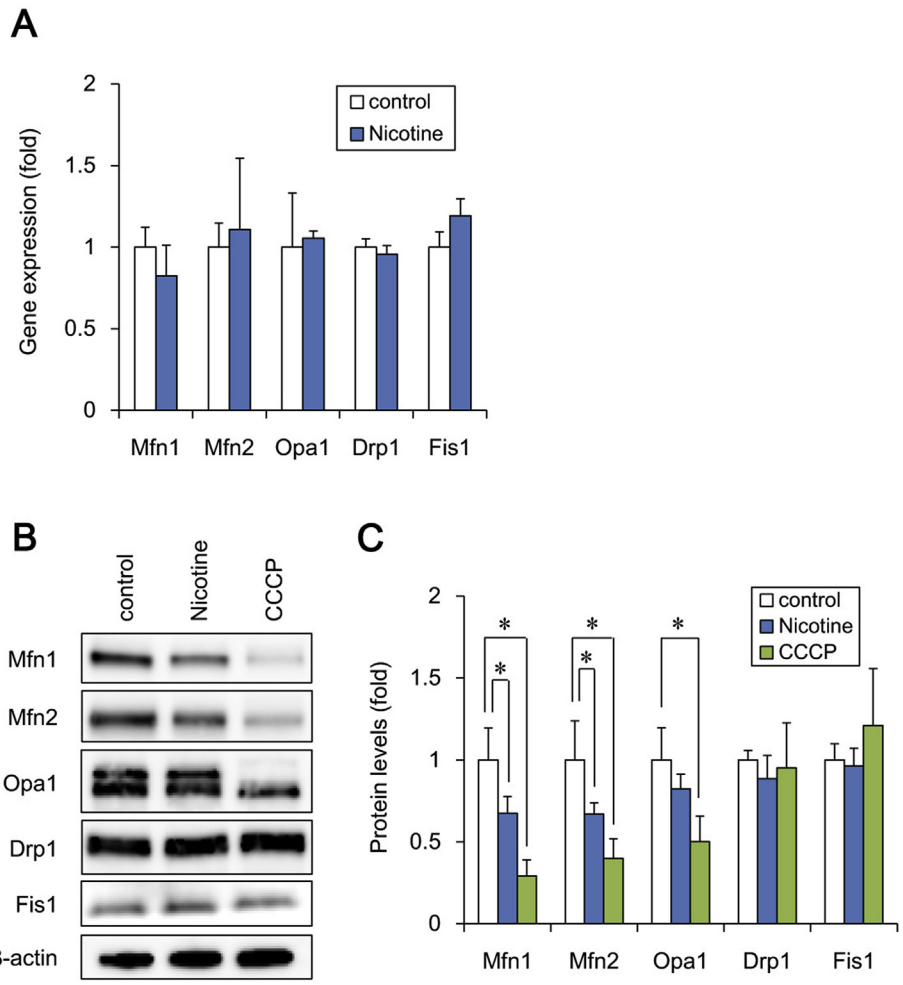

Fig. 4. Nicotine reduces Mfn1 and Mfn2 protein levels in NT2/D1 cells. A. After exposure to 10 μM nicotine for 24 h, the expression of the indicated mitochondrial genes was analyzed by real-time PCR. The relative changes were determined by normalizing with GAPDH. B. After exposure to 10 μM nicotine or 10 μM CCCP for 24 h, the expression of mitochondrial proteins was analyzed by western blot using anti-Drp1, anti-Fis1, anti-Mfn1, anti-Mfn2, anti-Opa1, or anti-β-actin antibodies. C. The band densities were analyzed by ImageJ software. Relative changes in expression were determined by normalization to β-actin. Data represent the mean ± SD (n = 3). *P < 0.05.

to cause mitochondrial fission via Mfn degradation. For example, organotin compounds such as tributyltin induce proteasomal degradation of Mfn1 and Mfn2, which facilitates mitochondrial fragmentation and growth arrest in NT2/D1 cells [30,31]. Since nicotine showed similar effects in NT2/D1 cells, nicotine exposure may also degrade Mfn1 and Mfn2 via proteasome. Moreover, an inhibitor of mitochondrial calcium efflux, CGP37157, is reported to degrade Mfn1 via E3 ubiquitin ligase and induce mitochondrial fission in prostate cancer LNCaP cells [32]. Further studies will be necessary to determine whether ubiquitin ligases are involved in nicotine-induced Mfn1 and Mfn2 degradation in embryonic cells.

Our data suggest that nicotine toxicity is mediated by dysfunctional mitochondrial quality control, which occurs via a nAChR-dependent mechanism (Figs. 2 and 3). Nicotine has been reported to evoke extracellular calcium influx through plasma membrane nAChRs [4]. Moreover, a transient increase in intracellular calcium levels is known to cause mitochondrial calcium overload, which is followed by the depolarization of the mitochondrial membrane, resulting in a loss of MMP [33,34]. In other cell lines, MMP reduction is reported to induce the mitochondrial translocation of the E3 ubiquitin ligase, Parkin, which targets the Mfn protein for proteasomal degradation [35]. Therefore, nicotine may increase intracellular calcium entry via nAChRs, thus reducing the MMP and inducing mitochondrial translocation of E3 ubiquitin ligases; this increases the proteasomal degradation of Mfn1 and Mfn2. Several reports indicate that knockdown of Mfn1 and Mfn2 in the cells induces mitochondrial fragmentation and shows severe cellular defects, including decreased ATP content and poor cell growth [36,37]. Especially, Mfn2 has been reported to be necessary for striatal axonal projections of midbrain dopamine neurons by the studies using dopamine neuron-specific Mfn2 knockout mice [38]. Taken together, Mfn1 and Mfn2 might be involved in several nAChR-mediated effects of nicotine, such as the reduction of ATP content, growth inhibition, and modulation of synaptic transmission. In future studies, it will be necessary to investigate the precise mechanism involved in nicotine-induced Mfn degradation, which results in mitochondrial fission and impaired function.

Conflict of interest

The authors declare that there are no conflicts of interest.

Acknowledgments

This work was supported by a Health and Labour Sciences Research Grant from the Ministry of Health, Labour and Welfare,

Japan (#H25-Kagaku-Ippan-002 to Y. Kanda), a Grant-in-Aid for Scientific Research from the Ministry of Education, Culture, Sports, Science, and Technology, Japan (#26293056, #26670041 to Y. Kanda), the Research on Regulatory Harmonization and Evaluation of Pharmaceuticals, Medical Devices, Regenerative and Cellular Therapy Products, Gene Therapy Products, and Cosmetics from Japan Agency for Medical Research and development, AMED (to Y. Sekino), and a grant from the Smoking Research Foundation (Y. Kanda).

Transparency document

Transparency document related to this article can be found online at http://dx.doi.org/10.1016/j.bbrc.2016.01.063.

Appendix A. Supplementary data

Supplementary data related to this article can be found at http://dx.doi.org/10.1016/j.bbrc.2016.01.063.

References

[1] V.S. Knopik, Maternal smoking during pregnancy and child outcomes: real or spurious effect? Dev. Neuropsychol. 34 (2009) 1–36.
[2] C.M. Tiesler, J. Heinrich, Prenatal nicotine exposure and child behavioural problems, Eur. Child. Adolesc. Psychiatry 23 (2014) 913–929.
[3] B.M. Conti-Fine, D. Navaneetham, S. Lei, A.D. Maus, Neuronal nicotinic receptors in non-neuronal cells: new mediators of tobacco toxicity? Eur. J. Pharmacol. 393 (2000) 279–284.
[4] E.X. Albuquerque, E.F. Pereira, M. Alkondon, S.W. Rogers, Mammalian nicotinic acetylcholine receptors: from structure to function, Physiol. Rev. 89 (2009) 73–120.
[5] Y. Kanda, Y. Watanabe, Nicotine-induced vascular endothelial growth factor release via the EGFR-ERK pathway in rat vascular smooth muscle cells, Life Sci. 80 (2007) 1409–1414.
[6] N. Hirata, Y. Sekino, Y. Kanda, Nicotine increases cancer stem cell population in MCF-7 cells, Biochem. Biophys. Res. Commun. 403 (2010) 138–143.
[7] N.L. Benowitz, Pharmacology of nicotine: addiction, smoking-induced disease, and therapeutics, Annu. Rev. Pharmacol. Toxicol. 49 (2009) 57–71.
[8] J.B. Dwyer, S.C. McQuown, F.M. Leslie, The dynamic effects of nicotine on the developing brain, Pharmacol. Ther. 122 (2009) 125–139.
[9] C.L. Crowley-Weber, K. Dvorakova, C. Crowley, H. Bernstein, C. Bernstein, H. Garewal, C.M. Payne, Nicotine increases oxidative stress, activates NF-kappaB and GRP78, induces apoptosis and sensitizes cells to genotoxic/xenobiotic stresses by a multiple stress inducer, deoxycholate: relevance to colon carcinogenesis, Chem. Biol. Interact. 145 (2003) 53–66.
[10] J.E. Bruin, M.A. Petre, S. Raha, K.M. Morrison, H.C. Gerstein, A.C. Holloway, Fetal and neonatal nicotine exposure in wistar rats causes progressive pancreatic mitochondrial damage and beta cell dysfunction, PLoS One 3 (2008) e3371.
[11] R.J. Youle, A.M. van der Bliek, Mitochondrial fission, fusion, and stress, Science 337 (2012) 1062–1065.
[12] T. Koshiba, S.A. Detmer, J.T. Kaiser, H. Chen, J.M. McCaffery, D.C. Chan, Structural basis of mitochondrial tethering by mitofusin complexes, Science 305 (2004) 858–862.
[13] S. Cipolat, O.M. De Brito, B. Dal Zilio, L. Scorrano, OPA1 requires mitofusin 1 to promote mitochondrial fusion, Proc. Natl. Acad. Sci. U. S. A. 101 (2004) 15927–15932.
[14] E. Smirnova, L. Griparic, D.-L. Shurland, A.M. van der Bliek, Dynamin-related protein Drp1 is required for mitochondrial division in mammalian cells, Mol. Biol. Cell 12 (2001) 2245–2256.
[15] Y. Yoon, E.W. Krueger, B.J. Oswald, M.A. McNiven, The mitochondrial protein hFis1 regulates mitochondrial fission in mammalian cells through an interaction with the dynamin-like protein DLP1, Mol. Biol. Cell 23 (2003) 5409–5420.
[16] Y. He, K.W. Leung, Y. Ren, J. Pei, J. Ge, J. Tombran-Tink, PEDF improves mitochondrial function in RPE cells during oxidative stress, Investig. Ophthalmol. Vis. Sci. 55 (2014) 6742–6755.
[17] G.P. Leboucher, Y.C. Tsai, M. Yang, K.C. Shaw, M. Zhou, T.D. Veenstra, M.H. Glickman, A.M. Weissman, Stress-induced phosphorylation and proteasomal degradation of mitofusin 2 facilitates mitochondrial fragmentation and apoptosis, Mol. Cell 47 (2012) 547–557.
[18] S. Yamada, Y. Kotake, Y. Sekino, Y. Kanda, AMP-activated protein kinase-mediated glucose transport as a novel target of tributyltin in human embryonic carcinoma cells, Metallomics 5 (2013) 484–491.
[19] S. Yamada, Y. Kotake, Y. Demizu, M. Kurihara, Y. Sekino, Y. Kanda, NAD-dependent isocitrate dehydrogenase as a novel target of tributyltin in human embryonic carcinoma cells, Sci. Rep. 4 (2014) 5952.
[20] X. Fan, R. Hussien, G.A. Brooks, H_2O_2-induced mitochondrial fragmentation in C2C12 myocytes, Free Radic. Biol. Med. 49 (2010) 1646–1654.
[21] N. Hirata, S. Yamada, T. Shoda, M. Kurihara, Y. Sekino, Y. Kanda, Sphingosine-1-phosphate promotes expansion of cancer stem cells via S1PR3 by a ligand-independent Notch activation, Nat. Commun. 5 (2014) 4806.
[22] Y. Kanda, T. Hinara, S.W. Kang, Y. Watanabe, Reactive oxygen species mediate adipocyte differentiation in mesenchymal stem cells, Life Sci. 89 (2011) 250–258.
[23] M.V. Skok, R. Grailhe, F. Agenes, J.P. Changeux, The role of nicotinic receptors in B-lymphocyte development and activation, Life Sci. 80 (2007) 2334–2336.
[24] L.M. Koval, A.S. Zverkova, R. Grailhe, Y.N. Utkin, V.I. Tsetlin, S.V. Komisarenko, M.V. Skok, Nicotinic acetylcholine receptors alpha4beta2 and alpha7 regulate myelo- and erythropoiesis within the bone marrow, Int. J. Biochem. Cell Biol. 40 (2008) 980–990.
[25] N. He, Z. Wang, Y. Wang, H. Shen, M. Yin, ZY-1, a novel nicotinic analog, promotes proliferation and migration of adult hippocampal neural stem/progenitor cells, Cell Mol. Neurobiol. 33 (2013) 1149–1157.
[26] C.N. Guo, L. Sun, G.L. Liu, S.J. Zhao, W.W. Liu, Y.B. Zhao, Protective effect of nicotine on the cultured rat basal forebrain neurons damaged by β-Amyloid (Aβ)25-35 protein cytotoxicity, Eur. Rev. Med. Pharmacol. Sci. 19 (2015) 2964–2972.
[27] Q. Liu, B. Zhao, Nicotine attenuates beta-amyloid peptide-induced neurotoxicity, free radical and calcium accumulation in hippocampal neuronal cultures, Br. J. Pharmacol. 141 (2004) 746–754.
[28] T. Zdravkovic, O. Genbacev, N. LaRocque, M. McMaster, S. Fisher, Human embryonic stem cells as a model system for studying the effects of smoke exposure on the embryo, Reprod. Toxicol. 26 (2008) 86–93.
[29] E.R. Gritz, V. Baer-Weiss, N.L. Benowitz, M.E. Van VunakisHjarvik, Plasma nicotine and cotine concentrations in habitual smokeless tobacco users, Clin. Pharmacol. Ther. 30 (1981) 201–209.
[30] S. Yamada, Y. Kotake, M. Nakano, Y. Sekino, Y. Kanda, Tributyltin induces mitochondrial fission through NAD-IDH dependent mitofusin degradation in human embryonic carcinoma cells, Metallomics 7 (2015) 1240–1246.
[31] M. Asanagi, S. Yamada, N. Hirata, H. Itagaki, Y. Kotake, Y. Sekino, Y. Kanda, Tributyltin induces G2/M cell cycle arrest via NAD^+-dependent isocitrate dehydrogenase in human embryonic carcinoma cells, J. Toxicol. Sci. (2016) in press.
[32] V. Choudhary, I. Kaddour-Djebbar, R. Alaisami, M.V. Kumar, W.B. Bollag, Mitofusin 1 degradation is induced by a disruptor of mitochondrial calcium homeostasis, CGP37157: a role in apoptosis in prostate cancer cells, Int. J. Oncol. 44 (2014) 1767–1773.
[33] M.R. Duchen, Mitochondria and calcium: from cell signalling to cell death, J. Physiol. 529 (2000) 57–68.
[34] N. Demaurex, D. Poburko, M. Frieden, Regulation of plasma membrane calcium fluxes by mitochondria, Biochim. Biophys. Acta 1787 (2009) 1383–1394.
[35] A. Tanaka, M.M. Cleland, S. Xu, D.P. Narendra, D.F. Suen, M. Karbowski, R.J. Youle, Proteasome and p97 mediate mitophagy and degradation of mitofusins induced by Parkin, J. Cell Biol. 191 (2010) 1367–1380.
[36] H. Chen, A. Chomyn, D.C. Chan, Disruption of fusion results in mitochondrial heterogeneity and dysfunction, J. Biol. Chem. 280 (2005) 26185–26192.
[37] W. Yue, Z. Chen, H. Liu, C. Yan, M. Chen, D. Feng, C. Yan, H. Wu, L. Du, Y. Wang, J. Liu, X. Huang, L. Xia, L. Liu, X. Wang, H. Jin, J. Wang, Z. Song, X. Hao, Q. Chen, A small natural molecule promotes mitochondrial fusion through inhibition of the deubiquitinase USP30, Cell Res. 24 (2014) 482–496.
[38] S. Lee, F.H. Sterky, A. Mourier, M. Terzioglu, S. Cullheim, L. Olson, N.G. Larsson, Mitofusin 2 is necessary for striatal axonal projections of midbrain dopamine neurons, Hum. Mol. Genet. 21 (2012) 4827–4835.

〈レクチャー6-3〉ファーマコビジランス

ヒトiPS細胞を用いた心毒性試験の現状と課題

諫田　泰成
国立医薬品食品衛生研究所・薬理部第二室

1．はじめに

ヒトiPS細胞の心毒性試験は、モデルとなる分化細胞を作製して医薬品候補化合物のスクリーニングを*in vitro*アッセイ系で評価することになるので、ヒト心筋を反映するような分化心筋細胞が大量かつ安定的に供給されることが必要不可欠である。現在、ヒトiPS細胞には株間の差など様々なバリエーションが存在することが明らかになっていることから[1]、分化誘導した心筋細胞にも未分化iPS細胞と同様にバラつきがあると考えられる。しかしながら、分化心筋細胞の品質基準などは定まっておらず、アカデミアやメーカーにおいてそれぞれバラバラの細胞を用いてアッセイを行っている可能性がある。インハウスの試験法を行う場合には問題はないが、安全性試験を実施するためには一定の評価基準が必要である。幹細胞由来の分化細胞は培養期間によっても性質が変化しうることが分かってきており、株化細胞やhERGを過剰発現させたHEK293細胞などのように扱うことができない。従って、いかに分化心筋細胞の品質を確保するのかが重要である。

本稿では、ヒトiPS細胞から心筋細胞への分化誘導技術ならびにiPS由来分化心筋細胞の薬理学的な特性を概説し、今後、医薬品による催不整脈作用に対する応用可能性、さらにはICHガイドラインへの展望について議論したい。

2．医薬品による催不整脈作用

医薬品によって発生する副作用の中で、トルサード・ド・ポアント（TdP）とよばれる重篤な不整脈は重要である[2]。発生頻度は極めて少ないものの心室細動に移行し突然死に至る症例が報告されており、上市後に販売が中止になった医薬品も少なくない。TdPはQT間隔の延長を伴うことから、TdP誘発リスクは、非臨床試験として*in vitro*でカリウム電流（hERGチャネル）阻害作用および*in vivo*で動物におけるQT延長作用を評価し（S7Bガイドライン）、臨床においてThorough QT/QTc試験を実施して厳密にヒトのQT間隔に対する作用を調べて（E14ガイドライン）、総合的にTdP誘発リスクを評価している。これらのガイドラインが整備された後は薬剤性心毒性の大きな問題は起きていないことから、一定のリスク評価ができていると考えられる。しかしながら、hERG試験で有用な医薬品候補化合物を落としてしまうこと、逆にhERGだけでは拾えない不整脈作用があることなどが指摘され、さらに予測性の高い試験系が求められている。iPS由来分化心筋細胞はヒト細胞でありマルチチャネルに対する評価が可能であることから[3]、hERG試験よりも予測性が向上するのではないか、あるいは臨床試験を削減できるのではないか、との期待が寄せられている。

3．ヒトiPS細胞を用いた心筋分化誘導法

ヒトiPS細胞を効率よく心筋分化する方法として、定方向分化誘導法が知られている[3,4]。**図1**に示すように、ヒトiPS細胞にサイトカインや増殖因子などを用いることにより、中胚葉、心筋前駆細胞、心筋細胞と段階的に分化誘導を行い、分化誘導後2週間ほどで自律的な拍動が観察される。このように作成されたiPS由来分化心筋細胞は個々の心筋細胞の活動電位の波形がバラバラである上に、電気生理学的に未成熟である。実際、201B7株から作製した分化心筋細胞も米国Cellular Dynamics International Inc.（CDI）から販売されているiCell心筋細胞も静止膜電位は-50mV程度と浅い（通常-90mV程度）。従って、未成熟な特性は元のiPS細胞株や分化誘導法に依存せず、iPS由来分化心筋細胞に共通の課題であることが示唆される。

そこで、心筋の成熟化を促進するためのアプローチとして、電気刺激など様々な手法が検討されてい

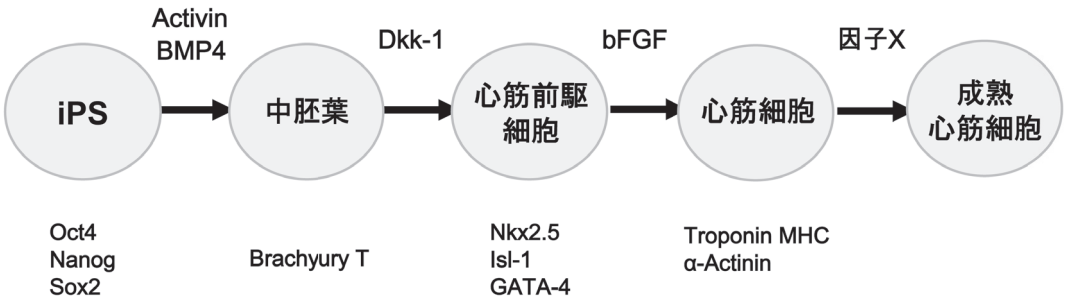

図1　ヒトiPS細胞から成熟心筋細胞の分化誘導法
ヒトiPS細胞からサイトカインなどの液性因子や遺伝子導入などの方法を用いて、段階的に心筋細胞に分化誘導できる。

る[5]。我々は成体心室筋と比較してiPS由来分化心筋細胞において不足している因子Xに着目し、心筋細胞の成熟化を誘導できる方法を明らかにしている（論文投稿中）。我々が検討した範囲では、アデノウイルスは未分化iPS細胞よりも分化が進んだ細胞の方が高い感染効率を示したことから、iPS由来分化心筋細胞にアデノウイルスを用いて因子Xを遺伝子導入することにより、成熟心筋を誘導することに成功した。ただし、医薬品の催不整脈作用を評価する上で成熟心筋の方がいいのかはまだ分かっていない。一般的にはヒト成体の心筋細胞に近ければ近い方が創薬のモデルとして良さそうであるが、本当に成熟した特性が必要なのかは以下に述べるような薬理作用の観点から判断すべきであろう。

4. 分化心筋細胞を用いた*in vitro*心毒性試験

*In vitro*心毒性試験に用いるiPS由来分化心筋細胞の形状としては、個々の細胞、EBなどの細胞塊、高密度培養によるシート状の標本などがあげられる。個々の細胞の場合は、パッチクランプで一つ一つの細胞の活動電位の波形をもとにQT間隔を評価するため、心室筋などのサブタイプの情報も得られる。しかしながら、スループット性は極めて低いこと、個々の細胞のバラつきの問題があること、長時間曝露による薬理作用も検討できないことなど多くの問題があり、現実的ではないように思われる。

一方、細胞塊やシート状の標本に関しては、多点電極システムを用いて、電極を埋め込んだディッシュに細胞塊やシートを接着させることによりQT間隔に相当する細胞外電位（Field Potential：FP）の測定が可能である。個々の心筋細胞のバラつきが平均化されるため、比較的安定したデータが得られること、侵襲がないため長時間曝露による薬理作用が調べられること、電気生理学特有の敷居の高さはなく比較的簡便であることなど、先程の問題点はかなり克服できる。我々が検討した範囲では、細胞塊は電極の上にうまく乗せられなかったり、細胞塊と電極の接触が不十分でシグナルが得られないようなケースがあったことから、シート状の標本の方がベターではないか、と考えている。ただし、多点電極システムを用いるにしても、一日で解析できる数に限界があり、大規模な医薬品候補化合物のスクリーニングには向いていない。今後、スループット性を上げるために改良が必要である。

我々は、iPS由来分化心筋細胞を用いた試験系の検出感度を明らかにするため、シート状に播種したiCell心筋細胞をモデル細胞として用いて、細胞外電位装置による評価を行った[6]。産官学の3施設で検証した結果、どの施設においてもhERG阻害剤E-4031の添加により濃度依存的にFPD（Field Potential Duration）延長が観察された（**図2**）。さらに、E-4031によりEarly afterdepolarization（EAD）やtriggered activityなどの異常な波形を検出できることが明らかになった（**図3**）。こちらはFPDとは異なり、既存の*in vitro*評価系では検出できないような不整脈のリスク評価につながると考えられ、非常に興味深い。現在、我々は成熟した分化心筋細胞を用いて同様のアッセイを行っており、催不整脈作用の評価に成熟心筋の特性が必要なのか明らかにする予定である。

今後、多点電極システムを用いた試験法の確立に向けて大規模なバリデーションを実施する場合、様々な実験条件を揃える必要がある。例えば、自律拍動なのかペーシングなのか、細胞の播種密度や培養期間、FPDの解析パラメーターの選択、EADの波形基準などがあげられる。特に、EADにおいては統一的な波形の判定基準の見解が得られていないので、波形の目合わせを行って情報を共有しながら

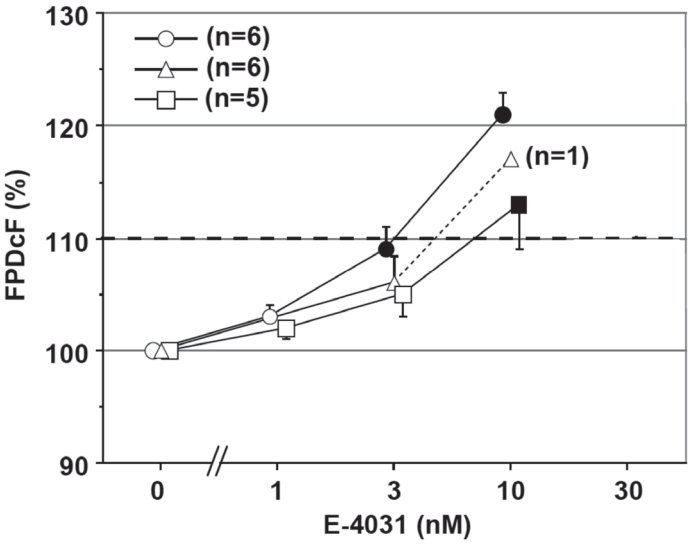

図2　E-4031によるFPD延長
各施設において、hERG阻害剤E-4031によってFPDの延長が認められた。

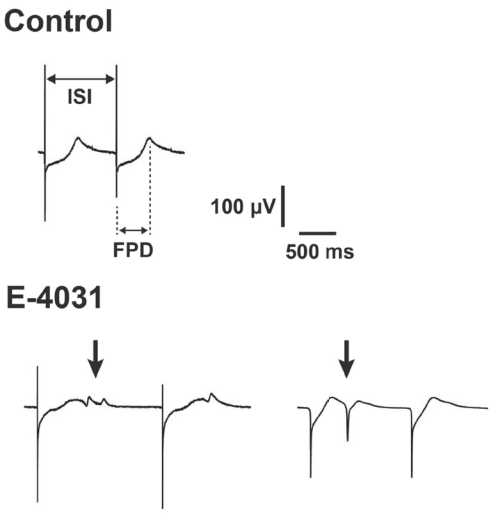

図3　E-4031による異常波形
E-4031によって、Triggered activityやEarly afterdepolarizationなどの異常な波形が認められた。

設定する必要があると思われる。

なお、今回は多点電極のデータを紹介したが、それ以外にも膜電位感受性色素やカルシウムイメージング、心収縮など様々な薬理評価法があり、陽性対照物質、陰性対照物質などのデータをもとに再現性や信頼性を評価していく必要がある。2013年に発足した製薬協タスクフォース(TF-5)においても様々な検証が行われており、今後の解析を待ちたい。

5. ガイドラインに向けた展望

ここ数年、ヒトiPS細胞を使った心毒性試験に関する発表が相次ぎ、iPS由来分化心筋細胞が催不整脈作用の評価に使えるのではないか、という機運が高まってきている。さらに、2013年7月から、FDA/HESI/CSRC*においてCiPA (Comprehensive *in vitro* Proarrhythmia Assay) の枠組みが発足し、薬剤による不整脈誘発リスク評価に関して国際的な議論も開始された[7,8]。特に、S7Bガイドラインの改定やE14ガイドラインの廃止などを見据えることを明言している。現在市販されている分化心筋細胞はメーカーの差やロット差等があるとされるが、良い細胞がないから議論できない、では全く前に進まないので、発想を変えて、今ある細胞で何ができるのか？を考える時期に来ている。日本としても、国内におけるiPS由来分化心筋細胞の大量かつ安定な供給体制を整備するとともに、多くの薬剤に対する心毒性データを揃えて、国際協調をはかりながらiPS細胞の実用化をすすめていく必要がある。

6. まとめ

ヒトiPS細胞の分化誘導技術などの研究が進展し、またCiPAなどの国際的な議論も開始されたことにより、ヒトiPS細胞を心毒性試験に利用する機運が高まってきている。日本としても、ガイドライン化を見据えて科学的な根拠をしっかりと確保しておかなければならない。将来的には、日本発のヒトiPS細胞技術を用いて、心毒性の発生を回避することが可能となり、より安全な医薬品が提供されることを期待したい。

7. 謝辞

本研究は、国立医薬品食品衛生研究所薬理部　関野祐子先生、東京医科歯科大学難治疾患研究所生体情報薬理分野　古川哲史先生　黒川洵子先生、東邦大学医学部薬理学講座　杉山篤先生　安東賢太郎先生　中村裕二先生、エーザイ株式会社　澤田光平先生　宮本憲優先生、株式会社新日本科学　松尾純子先生との共同研究です。深く感謝申し上げます。また、2014年1月に開催された第1回心臓安全性に関するシンクタンクミーティング2014 in 霧島に参加

* FDA：Food and Drug Administration
HESI：Health and Enviromental sciences Institute
CSRC：Cardiac Safety Research Consortium

された方々との討論も大変参考になりました。この場をお借りして感謝申し上げます。

参考文献

1) Bock C, Kiskinis E,et al：Reference Maps of human ES and iPS cell variation enable high-throughput characterization of pluripotent cell lines. Cell 2011.144.439-452.
2) Ferri N, Siegl P,et al：Drug attrition during pre-clinical and clinical development: understanding and managing drug-induced cardiotoxicity. Pharmacol Ther 2013.138.470-84.
3) Burridge PW, Keller G,et al：Production of de novo cardiomyocytes: human pluripotent stem cell differentiation and direct reprogramming. Cell Stem Cell 2012.10:16-28.
4) Uosaki H, Fukushima H, et al：Efficient and scalable purification of cardiomyocytes from human embryonic and induced pluripotent stem cells by VCAM1 surface expression. PLoS ONE 2011;6:e23657.
5) Lieu DK, Fu JD, et al: Mechanism-based facilitated maturation of human pluripotent stem cell-derived cardiomyocytes. Circ Arrhythm Electrophysiol 2013.6.191-201.
6) Nakamura Y, Matsuo J, et al：Assessment of testing methods for drug-induced repolarization delay and arrhythmias in an iPS cell-derived cardiomyocyte sheet: multi-site validation study. J Pharmacol Sci 2014.124.494-501.
7) Chi KR. Revolution dawning in cardiotoxicity testing. Nat Rev Drug Discov 2013.12.565-567.
8) Sager PT, Gintant G, et al：Rechanneling the cardiac proarrhythmia safety paradigm:a meeting report from the Cardiac Safety Research Consortium. Am Heart J 2014.167.292-300.

再生医療における臨床研究と製品開発

諫田　泰成

国立医薬品食品衛生研究所 薬理部第二室 室長

(株)技術情報協会

「再生心筋細胞を用いた安全性薬理評価系の開発」　抜刷

2013年9月発刊

第 3 節　再生心筋細胞を用いた安全性薬理評価系の開発

はじめに

ヒト iPS 細胞は，今まで入手が困難であったヒト細胞の作製が可能となるため，「再生医療」と「創薬」の実用化が期待されている（図 1）。再生医療への注目度は非常に高く，ヒト iPS 細胞から作成した網膜色素上皮細胞を移植する臨床研究が 2012 年度に申請され，正式に承認された。創薬応用としては，医薬品の安全性や有効性の評価に対する利用が考えられ，創薬プロセスの早い段階で医薬品候補化合物の副作用などを予測できれば，臨床試験における予測性の向上や安全性確保，開発コスト削減などが期待される（図 1）。

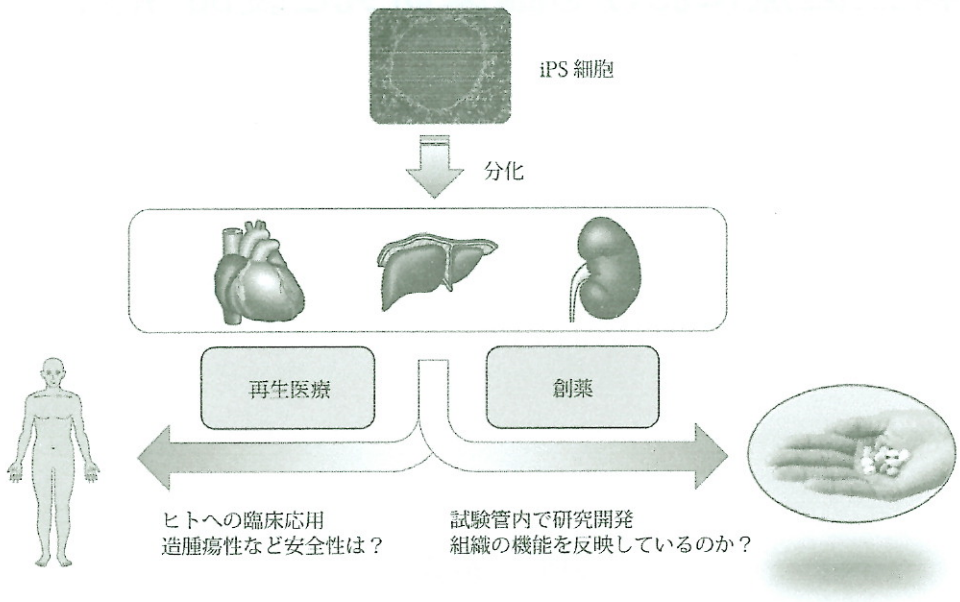

図 1　ヒト iPS 細胞の医療応用への可能性

これらのヒト iPS 細胞の実用化に向けた課題として，ヒト未分化 iPS 細胞の品質，すなわち株間の差，継代数や研究室間の差などが明らかになり，国内外のプロジェクトにより標準化の作業が進められている[1]。しかし，ヒト iPS 細胞由来の分化細胞に関してはほとんど標準化が手付かずであり，分化誘導の標準プロトコールや分化細胞の品質評価，分化指向性などあまり明らかになっていない。

また，再生医療と創薬応用でそれぞれ克服すべき課題も明らかになってきている。再生医療においては，分化細胞の安全性の確保が必須であり，残存している未分化 iPS 細胞の検出など造腫瘍性の評価法の開発が進められている[2]。分化心筋細胞に関しては，移植によって不整脈が誘発されないかなどの検証も必要である。創薬応用は，in vitro のアッセイ系で分化細胞を使用するため再生医療とは異なり安全面のハードルが低く分化製品に対するウイルス導入などの加工も可能であるが，元の臓器の性質を反映した成熟した細胞が必要と考えられる。

そこで本稿では，ヒト iPS 細胞から心筋細胞への分化誘導技術ならびに分化心筋細胞の電気生理学的特性を概説し，将来的にヒト iPS 細胞の創薬応用実用化に向けて整備すべき課題について考察したい。

1.　ヒト iPS 細胞の心筋分化誘導法

1.1　EB 形成法

ヒト iPS 細胞から分化心筋細胞の一般的な作製法として，図 2A に示すような胚様体（Embryoid body, EB）を形成させる方法が知られている。胚の発生過程を in vitro で模倣するためにマウス ES 細胞から擬似的な胚である EB を形成さ

せる方法が開発され，ヒト iPS 細胞にも応用されている。

マウス ES 細胞の場合には，未分化 ES 細胞をトリプシン処理により single cell にして，非接着コート処理済の 96 ウエルプレートなどを用いて EB を形成する。一方，ヒト iPS 細胞の場合には single cell にすると細胞死が起きるため，最初は小さな細胞塊を用いて EB を作成する必要がある。小さな細胞塊はヒト iPS 細胞のコロニーを CTK 溶液（トリプシン，コラーゲナーゼを含む分散液）などで処理した後ピペッティングすることによって作製し，低接着ディッシュに移す。すぐに 10% 血清を含む DMEM などの分化培地に変更すると細胞死が誘導されることがあるため，我々は basic fibroblast growth factor（bFGF）を含む未分化維持培地で数日間培養して EB を形成させてから，3 日ごとに半量を分化培地（10% 血清，0.1mM 2- メルカプトエタノール，非必須アミノ酸を添加した DMEM）に切り替えている。未分化維持に重要な bFGF の除去により分化スイッチが ON になり，外・中・内胚葉の三方向へ分化が誘導される。中胚葉を経由して心筋にも分化が誘導され，分化培地で EB の培養を続けると 2 ～ 3 週間後に拍動する EB が観察される。

EB 法の欠点は，三方向へ分化が誘導されるため，特定の細胞への分化効率が低いことである。EB の中でも心筋細胞は 10% 程度しか含まれていない。そこで，心筋分化効率を高くするために分化を亢進する液性因子が探索され，BMP-4，Wnt3a，G-CSF など様々な因子が報告されている[3-5]。もう一つの欠点は，EB のサイズが不均一で形状もばらばらであるため，EB 間の差が大きく拍動数などもバラつくことである。我々は EZ passage（Invitrogen #23181-010）を使用してコロニーを処理し，できる限り均一なサイズとなるように心掛けている。最近，V 字型ウエルの中で強制的に EB を形成させるプレートがいくつか報告されており，形やサイズのそろった EB 作成法の開発が期待される。

このように EB 形成を介する分化プロトコールは比較的簡便であり，特別な試薬を用いることなく血清を含む培地で分化誘導も可能であるが，問題点として，ヒト iPS 細胞には分化指向性が存在し，株間で心筋分化能に差が認められることがあげられる。公的な細胞バンクから入手可能な株の中で，201B7 株，253G1 株は心筋分化能が高いが，Tic 株（JCRB1331）はほとんど拍動が認められないことから，ヒト iPS 細胞には分化の方向性を規定する特性（分化指向性）があると考えられる。Tic 株は肝臓への分化効率が高いと報告されており[6]，心筋に対しては分化抵抗性を有する可能性がある。分化指向性に関するメカニズムや選別のマーカーなどは明らかになっていないので，今後の研究の進展が待たれる。目的に応じて最適なヒト iPS 細胞株を入手できるように、分化特性も含めた細胞バンクの整備が望まれる。また、そのような情報を共有するシステムも必要である。

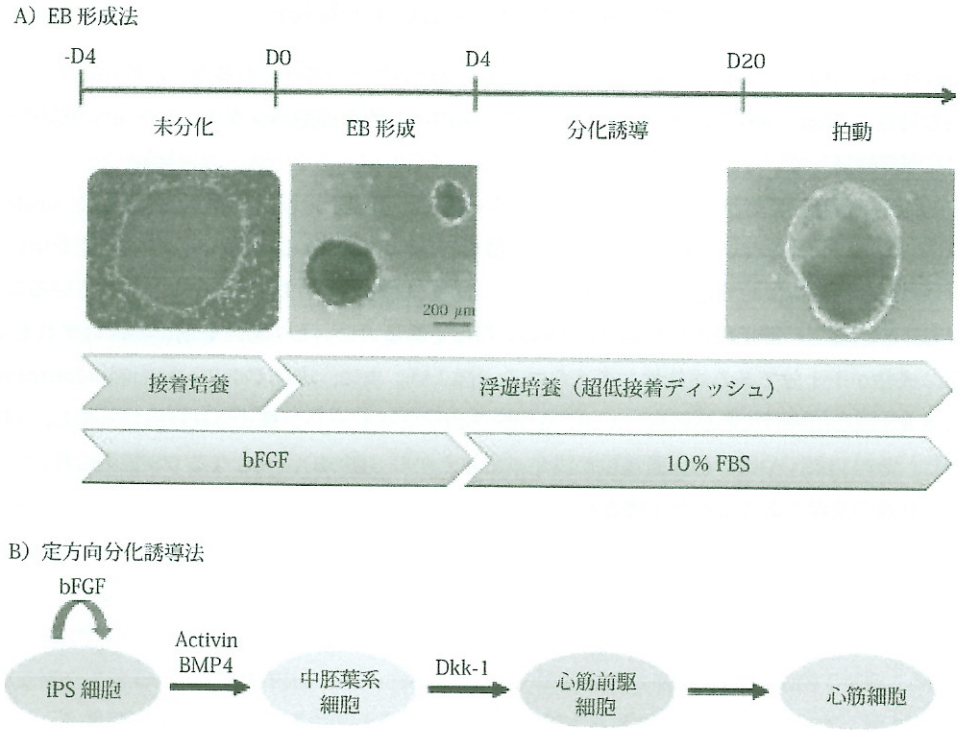

図 2　ヒト iPS 細胞の心筋分化誘導法

1.2 定方向分化誘導法

定方向分化誘導法とは，液性因子などを用いて特定の方向へ分化を特徴付ける方法であり，心筋細胞の場合は，中胚葉⇒心筋前駆細胞⇒心筋細胞，と段階的に分化誘導を行うことを指す（図 2B）。この際，各ステップで添加する液性因子は，心筋細胞の発生過程や ES 細胞由来分化細胞に発現している受容体などを元にして，液性因子のスクリーニングや最適化が行われている[7]。

まず，ヒト iPS 細胞をマトリゲルでコートしたディッシュに高密度で播種して，数回継代を行うことによりフィーダーをできる限り除去した後，Activin により中胚葉や内胚葉の元となる原条へ分化誘導する。BMP-4 の添加により中胚葉へ分化誘導がかかる。次に，Wnt antagonist である Dickkopf-1（Dkk-1）などにより心筋前駆細胞の方向へ分化を行い、最終的には心筋細胞の拍動が観察される。

EB 形成法と比較すると，定方向分化誘導法は拍動までの期間が約 1 週間と顕著に短縮できる特徴がある。実際，酵素処理により分散しトロポニンで染色すると 40% 以上の細胞が心筋細胞であることから，分化効率も非常に高いことを確認している。また，接着したまま分化誘導を行うのでシートのような状態となり，ダイナミックな拍動が観察できる。欠点は，分化誘導のステップが増えて EB 形成法よりも手間とコストがかかること、ヒト iPS 細胞のコロニーの密度により分化効率が大きく異なることなどがあげられる。また，添加する因子は濃度に加えてタイミングも重要である。Wnt シグナルは心筋分化の初期には促進的に作用し，後期では抑制的に作用することが知られており、タイミングが合わない場合には全く逆の作用をもたらすことが起こり得る。従って，液性因子を添加する時期・濃度・順序などに関して慎重に最適化する必要がある。

このように心筋細胞への分化プロトコールは EB 法，定方向分化法ともに改良が加えられてきているが，分化心筋細胞における遺伝子発現やイオンチャネルの発現は幼若タイプである[8,9]。後述するように、分化心筋細胞は電気生理学的にも未成熟であるため，現在，我々は成熟させる分化誘導法を構築中である（投稿準備中）。再生医療においては細胞移植により心機能が回復するのかが焦点となるので分化細胞の成熟度はあまり問題にならず，むしろ液性因子の産生が重要と言われているが，創薬応用の場合は成熟度が薬剤のスクリーニング効率に影響をあたえる可能性があり，今後の研究に進展が期待される。

2. 分化心筋細胞の電気生理学的な特性

一般的に細胞の特性の指標として遺伝子発現やマーカー分子の発現などがあげられるが，心筋細胞で最も重要なことは電気生理学的な特性である。筆者らは創薬応用に向けて，国内の公的な細胞バンクよりヒト iPS 細胞株を入手して，分化心筋細胞の品質を検証している。

201B7 株由来の拍動 EB をピンセットで引っ張るかカッターで刻んだ後にトリプシン処理をすると single cell を単離でき，ラミニンでコートしたディッシュに再播種すると拍動する細胞が得られる。この単離拍動細胞を用いてマニュアルパッチクランプにより活動電位を測定したところ，結節，心房，心室型の各サブタイプが存在していることが明らかになった。しかし，心筋細胞の静止膜電位が通常は -90mV 程度であるのに対して分化心筋細胞はいずれも -40mV 程度と浅いことから，成熟が不十分である可能性が考えられる（図 3A）。次に，米国 Cellular Dynamics International 社で販売されているヒト iPS 細胞由来分化心筋細胞（iCell）を iPS アカデミアジャパン株式会社経由で入手し，同様に活動電位の測定を行った。その結果，やはり静止膜電位が浅かったことから（図 3B），元となる iPS 細胞の株によるのではなく分化心筋細胞の共通の課題であることが示唆された。

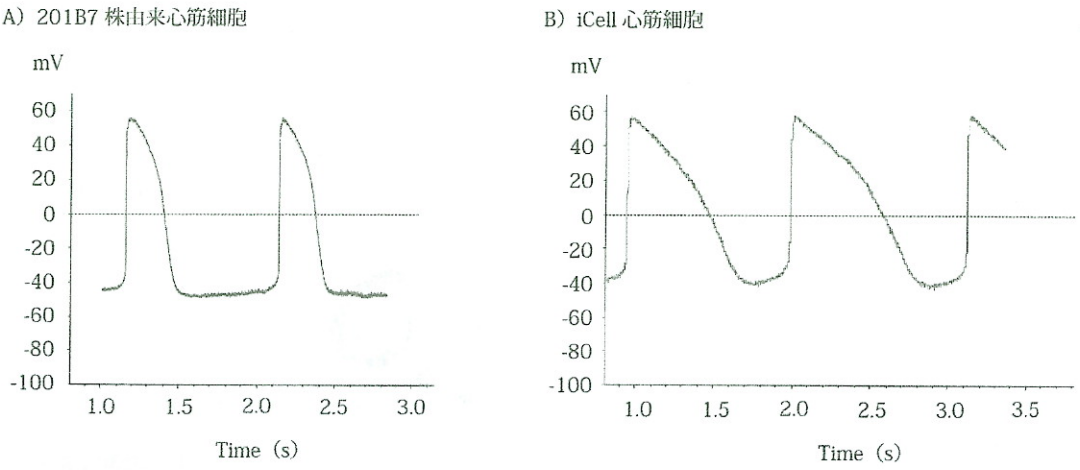

図3　分化心筋細胞の活動電位

このような分化心筋細胞を用いた薬理作用の評価においては，様々なヒトiPS細胞株から種々の手法を用いて心筋へ分化誘導すると，心筋細胞のサブタイプの割合や成熟度が不均一となり，薬剤に対する反応性についてもばらつくことが予想される。同一の化合物に対して同様の薬理作用が観察できない限り、催不整脈の予測が困難であり、バラつきを抑える必要がある。そこで，我々は次に述べるように，心筋シートを用いた実験プロトコールを整備している。

3.　分化心筋細胞を用いた安全性薬理試験

分化心筋細胞を用いた創薬応用の例として，薬剤性不整脈のリスク評価が考えられる。医薬品によって発生する副作用の中でもトルサード・ド・ポアント（TdP）とよばれる重篤な不整脈は重要で，発生頻度は極めて少ないもののまれに心室細動に移行し突然死に至る[10]。TdPはQT間隔（心室の興奮から再分極までの時間）の延長を伴うことから，現在TdPのリスクは，非臨床試験としてカリウムチャネル（IKr）を発現させたHEK293細胞を用いてカリウム電流阻害作用を検討し（hERG試験法），次いでin vivoで動物のQT延長作用を評価し，その後臨床においてThorough QT/QTc試験により厳密にヒトのQT間隔に対する作用を調べることにより，一定の評価が可能である（図5）。しかしながら，hERG試験法は疑陽性が多く，有用な化合物を化合物のスクリーニングのプロセスで除外してしまう可能性がある。ヒトiPS細胞由来の分化心筋細胞は，カリウム（IKs/IKr）に加えて，カルシウム，ナトリウムなど複数のチャネルが発現しているため再分極電流への影響を総合的に評価できる利点があり，疑陽性が減少して予測性が向上することが期待される。今までは，心筋への分化誘導条件（細胞株、分化誘導分化誘導法、日数，培養細胞密度など）が異なるばかりではなく，心筋細胞の電気生理学的機能の測定方法も異なっていたために，実験データを研究間で比較検討ができず，実験結果の再現性を確かめることが困難であった。そこで，我々は電気生理学的特性の解析法を比較検討し、不整脈検出プロトコルの標準化作業を行っている。

個々の心筋細胞の場合は，パッチクランプで解析が可能である。一つ一つの細胞の活動電位の波形をもとにQT間隔を評価するため，心筋細胞のサブタイプの情報も同時に得られる利点がある。さらに，QT延長などに起こることが多い早期後脱分極も直接検出することができる。しかし，前述したように個々の波形にバラつきが認められること，スループット性が低く大規模なスクリーニングには向かないこと，侵襲があるので短時間の薬理作用に限定されてしまうことなどを考慮すると，現実的には薬理作用の検出には向かないと考えられる。

細胞塊の場合は，図4Aに示すような多点電極システムを用いて心電図の解析が可能である。電極を埋め込んだディッシュに細胞塊を接着させると，細胞外電位（Field Potential; FP）が測定できる。FPは細胞内で記録される活動電位の微分波形に一致し，心電図によって得られる信号と同様の変化を記録する事ができる[11]。従って，ナトリウムによるピークから活動電位再分極時に観察されるカリウムのピークまでの時間であるFPDは，心電図におけるQT間隔に相当する。

FPD を用いる利点は，侵襲がないため医薬品候補化合物の長時間曝露による薬理作用が調べられることである。しかし，細胞塊ごとの FP の波形が一定の範囲内になるよう均一な塊の作製技術が必要不可欠である。さらに，EB が電極に接していなければシグナルが取得できない。もともと心筋細胞はガラスに張り付きにくい性質がある上に，拍動によってディッシュから剥がれたり接着場所が変わったりするので，ディッシュをコートする基材やデバイスの改善が求められる。我々が作製したヒト iPS 細胞由来の拍動 EB も市販のヒト ES 細胞由来細胞塊（スウェーデン Cellectis 社）も細胞外電位の測定に手間と時間がかかり，スループット性も低く，現時点では薬理作用の検出にはまだまだ遠いと言わざるを得ない。

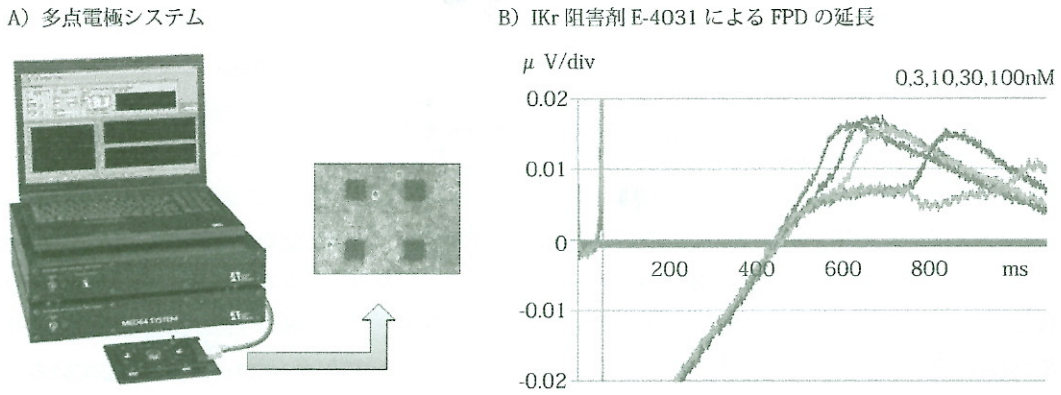

図 4　心筋シートにおける FP の解析

そこで，我々は心筋シートを用いて多点電極システムによる QT 延長評価系の開発に着手した。心筋シートは分化心筋細胞を密に播種することで容易に作成することができ同期した拍動が観察される。シート形成により EB 間や個々の心筋細胞などのバラつきが平均化されるため安定したデータが得られると期待される。また，シートは多点電極全体を覆うことになるので，FP のデータ取得も大幅に改善される。実際例として，陽性対照物質である IKr 阻害剤 E-4031 によって心筋シートの FPD 延長が検出できる（図 4B）。現在、産官学の枠組みで市販の分化心筋細胞を用いて、薬理作用の再現性，メーカの相違，ロット間差など比較を行っており、不整脈検出プロトコールの標準化を行っている。

最終的に、分化心筋細胞を用いた試験法として確立するためには，検出感度，再現性，信頼性などを検証する必要がある。検出感度に関しては，今のところ，分化心筋細胞を用いた評価系は感受性が高いような結果が得られており，hERG 試験で落とされた医薬品候補化合物を拾えるようなフォローアップに使用できるのかは不明である。再現性や信頼性を明らかにするためには，特定のラボ内のデータのみでは評価できないので，施設内及び多施設間で多くの化合物を用いたバリデーションを行う必要がある。本当に分化心筋細胞を用いる試験系が hERG 試験よりも優位性があるのか？分化心筋細胞の試験法が手間やコストをかけるだけの価値があるのか？ヒトにおける予測性が向上するのか？臨床試験を代替しうるのか？などを明らかにしなければならない。

おわりに

ヒト iPS 細胞の分化誘導技術などの研究の進展により，ヒト iPS 細胞の実用化に向けた動きが盛んである。創薬応用の実用化に向けては，ヒト iPS 細胞の株間の差，分化細胞の規格，安全性薬理試験のプロトコール整備など再生医療とは異なる多くの課題が残されている。薬剤性不整脈のリスク評価に関しては，現行の hERG 試験法に対する優位性も重要なポイントである。これらの課題を克服することにより、創薬プロセスの効率が向上し，将来的には承認審査の迅速化が実現することが期待される。

謝辞

本研究を遂行するにあたり，貴重なご助言とご指導を賜りました国立医薬品食品衛生研究所薬理部　関野祐子部長，東京医科歯科大学難治疾患研究所生体情報薬理分野　古川哲史教授，黒川洵子准教授，エーザイ株式会社　澤田光平博士，宮本憲優博士，株式会社 Ion Chat Research　齋藤光義博士に深く感謝申し上げます。

文　　献

1) Bock C, Kiskinis E, Verstappen G, Gu H, Boulting G, Smith ZD, Ziller M, Croft GF, Amoroso MW, Oakley DH, Gnirke A, Eggan K, Meissner A.Cell 144:439-452 (2011)

2) Kuroda T, Yasuda S, Kusakawa S, Hirata N, Kanda Y, Suzuki K, Takahashi M, Nishikawa S, Kawamata S, Sato Y.PLoS ONE 7:e37342 (2012)

3) Takei S, Ichikawa H, Johkura K, Mogi A, No H, Yoshie S, Tomotsune D, Sasaki K.Am J Physiol. 296:H1793-H1803 (2009)

4) Tran TH, Wang X, Browne C, Zhang Y, Schinke M, Izumo S, Burcin M.Stem Cells 27:1869-1878 (2009)

5) Shimoji K, Yuasa S, Onizuka T, Hattori F, Tanaka T, Hara M, Ohno Y, Chen H, Egasgira T, Seki T, Yae K, Koshimizu U, Ogawa S, Fukuda K.Cell Stem Cell 6:227-237 (2010)

6) Inamura M, Kawabata K, Takayama K, Tashiro K, Sakurai F, Katayama K, Toyoda M, Akutsu H, Miyagawa Y, Okita H, Kiyokawa N, Umezawa A, Hayakawa T, Furue MK, Mizuguchi H.MolTher. 19: 400-407 (2011)

7) Fujiwara M, Yan P, Otsuji TG, Narazaki G, Uosaki H, Fukushima H, Kuwahara K, Harada M, Matsuda H, Matsuoka S, Okita K, Takahashi K, Nakagawa M, Ikeda T, Sakata R, Mummery CL, Nakatsuji N, Yamanaka S, Nakao K, Yamashita JK.PLoS ONE, 6:e16734 (2011)

8) Beqqali A, Kloots J, Ward-van Oostwaard D, Mummery C, Passier R.Stem Cells, 24:1956-1967 (2006)

9) Cao F, Wagner RA, Wilson KD, Xie X, Fu JD, Drukker M, Lee A, Li RA, Gambhir SS, Weissman IL, Robbins RC, Wu JC.PLoS ONE, 3:e3474 (2008)

10) Yap YG and CammAJ.Heart 89:1363-1372 (2003)

11) Kamp TJ and January CT. Drug Discovery Today: Disease Mechanisms 1:45 (2004)